

University of New Hampshire
University of New Hampshire Scholars' Repository

Master's Theses and Capstones

Student Scholarship

Winter 2009

Characterization of T24D14(ok809) a putative alpha-1,2 glucosyltransferase in *C. elegans* and detailed structural analysis of the lipid linked oligosaccharide pathway via MSN

William Cobb Wiswall Jr.
University of New Hampshire, Durham

Follow this and additional works at: <https://scholars.unh.edu/thesis>

Recommended Citation

Wiswall, William Cobb Jr., "Characterization of T24D14(ok809) a putative alpha-1,2 glucosyltransferase in *C. elegans* and detailed structural analysis of the lipid linked oligosaccharide pathway via MSN" (2009). *Master's Theses and Capstones*. 505.
<https://scholars.unh.edu/thesis/505>

This Thesis is brought to you for free and open access by the Student Scholarship at University of New Hampshire Scholars' Repository. It has been accepted for inclusion in Master's Theses and Capstones by an authorized administrator of University of New Hampshire Scholars' Repository. For more information, please contact nicole.hentz@unh.edu.

CHARACTERIZATION OF T24D1.4(*ok809*) A PUTATIVE ALPHA-1,2
GLUCOSYLTRANSFERASE IN *C. ELEGANS*

AND

DETAILED STRUCTURAL ANALYSIS OF THE LIPID LINKED
OLIGOSACCHARIDE PATHWAY VIA MS^N

BY

William Cobb Wiswall Jr

B.S., Fairfield University, 2002

THESIS

Submitted to the University of New Hampshire
in Partial Fulfillment of the Requirements

for the Degree of

Master of Science

In

Biochemistry

December, 2009

UMI Number: 1481707

All rights reserved

INFORMATION TO ALL USERS

The quality of this reproduction is dependent upon the quality of the copy submitted.

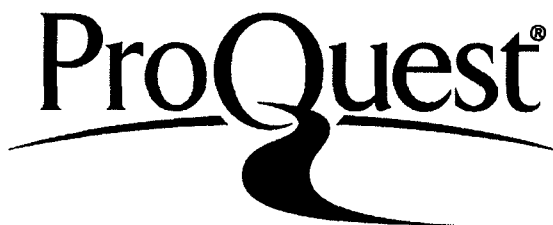
In the unlikely event that the author did not send a complete manuscript and there are missing pages, these will be noted. Also, if material had to be removed, a note will indicate the deletion.



UMI 1481707

Copyright 2010 by ProQuest LLC.

All rights reserved. This edition of the work is protected against unauthorized copying under Title 17, United States Code.



ProQuest LLC
789 East Eisenhower Parkway
P.O. Box 1346
Ann Arbor, MI 48106-1346

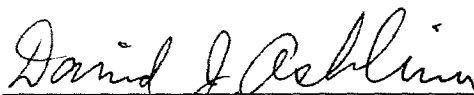
This thesis has been examined and approved.



Thesis Director, Vernon N. Reinhold,
Professor of Biochemistry and Molecular Biology



W. Kelley Thomas,
Professor of Biochemistry and Molecular Biology



David J. Ashline, Research Scientist

November 18, 2009

Date

DEDICATION
FOR MY MOM AND DAD

ACKNOWLEDGEMENTS

I would like to thank my advisor Vernon Reinhold for his support and guidance. I would also like to thank all my of my committee members for their helpful insight, especially Kelley Thomas and David Ashline. In addition, my sincere respect and appreciation goes to my colleagues Justin Prien and Weston Struwe. Their assistance and friendship were an integral part of my graduate experience at UNH.

I will be eternally grateful to my first advisor and friend Charles Warren who exemplified the true nature of a scientist. His zeal for life and research were contagious. He was an ideal mentor and I will never forget the knowledge he passed on to me.

Finally, I would like to extend my gratitude, appreciation and love to my parents. My late father, a pediatrician for over 50 years, was a paragon to me for all aspects of life. Our scientific discussions began when I was only child and he inspired me to study biology. My mother facilitated this greatly by often taking me on trips the Museum of Science in Boston. My mother was also extremely important as an unwavering source of encouragement and support for which I am so very thankful.

TABLE OF CONTENTS

DEDICATION.....	iii
ACKNOWLEDGEMENTS.....	iv
LIST OF TABLES.....	vii
LIST OF FIGURES.....	viii
ABSTRACT.....	xi

CHAPTER	PAGE
1. GLYCOPROTEIN BIOSYNTHESIS.....	1
1.1 Biochemistry of the Lipid Linked Oligosaccharide Pathway.....	4
2. CONGENITAL DISORDERS OF GLYCOSYLATION.....	8
2.1 Aberrant Glycosylation and Disease.....	11
3. USE OF C. ELEGANS AS A MODEL ORGANISM.....	12
4. CHARACTERIZATION OF T24D1.4(<i>OK809</i>).....	14
4.1 Protein Homology for T24D1.4.....	14
4.2 Specific Aims.....	17
4.3 Materials and Methods.....	17
4.4 Results.....	21
4.4.1 Calsequestrin Hypoglycosylation Blot.....	21
4.4.2 MALDI -TOF CFR of LLO Precursor Glycans.....	22
4.4.3 Phenotypic Analysis.....	24
4.5 Conclusions.....	29
4.6 FUTURE WORKS.....	31

5. COMPARATIVE STRUCTURAL ANALYSIS OF LIPID LINKED OLIGOSACCHARIDES IN C. ELEGANS AND MOUSE MACROPHAGE CELLS.....	32
5.1 Sequential Mass Spectrometry.....	34
5.2 Materials and Methods.....	35
5.3 Results.....	37
5.3.1 LLOs are not Substantially Degraded Upon Cell Lysis.....	37
5.3.2 Comparative Structural Analysis Man ₃ GlcNAc ₂ LLO	39
5.3.3 Comparative Structural Analysis Man ₄ GlcNAc ₂ LLO	47
5.3.4 Comparative Structural Analysis Man ₅ GlcNAc ₂ LLO	53
5.4 FUTURE DIRECTIONS.....	63
CONCLUSIONS.....	65
REFERENCES.....	69

LIST OF TABLES

Table 1. Congenital Disorders of Glycosylation Type I.....	9
Table 2. Wormbase gene homology report for T24D1.4.....	15
Table 3. Blast results from submitting the T24D1.4 protein sequence against the yeast protein database.....	16
Table 4. Blast results from submitting the yeast ALG10 protein sequence against the <i>C. elegans</i> protein database.....	16
Table 5. Egg laying deficiency assay.....	26
Table 6. Table of the MS ⁿ pathways analyzed for Man ₃ GlcNAc ₂ LLO and the corresponding topologies.....	47
Table 7. Table of the MS ⁿ pathways analyzed for Man ₄ GlcNAc ₂ LLO and the corresponding topologies.....	53
Table 8. Table of the MS ⁿ pathways analyzed for Man ₅ GlcNAc ₂ LLO and the corresponding topologies.....	62
Table 9. Table of the MS ⁿ pathways analyzed for Man ₅ GlcNAc ₂ LLO and the corresponding topologies.....	63

LIST OF FIGURES

Figure 1. Overview of glycoprotein biosynthesis.....	2
Figure 2. <i>N</i> -glycan types.....	3
Figure 3. Lipid Linked Oligosaccharide Pathway.....	5
Figure 4. ER and Golgi Processing.....	7
Figure 5. Amino acid sequence comparison of the predicted <i>C. elegans</i> T24D1.4 protein to the characterized yeast ALG10 protein.....	15
Figure 6. Calsequestrin western blot.....	21
Figure 7. Calsequestrin western blot.....	22
Figure 8. MALDI-TOF profile of wild type <i>C. elegans</i> LLO.....	23
Figure 9. MALDI-TOF profile of T24D1.4(<i>ok809</i>).....	23
Figure 10. Brood size assay.....	25
Figure 11. Generation time assay.....	27
Figure 12. Tunicamycin assay.....	28
Figure 13. Expected LLO Structure.....	33
Figure 14. Figure MALDI-TOF CFR profile of standard Glc ₃ Man ₉	38
Figure 15. MALDI-TOF CFR profile of LLO degradation assay.....	38
Figure 16. MS ⁴ pathway of the <i>m/z</i> 1187.6, Man ₃ GlcNAc ₂ LLO from <i>C.</i> <i>elegans</i>	40
Figure 17. MS ⁵ spectra of <i>m/z</i> 1187.6, Man ₃ GlcNAc ₂ LLO from <i>C. elegans</i>	41
Figure 18. MS ⁴ spectra of <i>m/z</i> 1187.6, Man ₃ GlcNAc ₂ LLO from <i>C. elegans</i>	42
Figure 19. MS ⁴ spectra of <i>m/z</i> 1187.6, Man ₃ GlcNAc ₂ LLO from <i>C. elegans</i>	43

Figure 20. MS ⁴ spectra of <i>m/z</i> 1187.6, Man ₃ GlcNAc ₂ LLO from mouse macrophage cells.....	44
Figure 21. Comparison of the MS ² spectra of the <i>m/z</i> 1187.6.....	45
Figure 22. MS ⁴ pathway of the <i>m/z</i> 1187 isolating the terminal HexNAc structure from mouse macrophage cells.....	46
Figure 23. MS ⁴ spectra of the <i>m/z</i> 1391.5 Man ₄ GlcNAc ₂ LLO from <i>C. elegans</i>	48
Figure 24. MS ⁵ of the <i>m/z</i> 1391.5, Man ₄ GlcNAc ₂ LLO from <i>C. elegans</i>	49
Figure 25. Comparison of the MS ² spectra of the <i>m/z</i> 1391.5.....	50
Figure 26. MS ⁴ of the <i>m/z</i> 1391.5, Man ₃ GlcNAc ₂ LLO from mouse macrophage cells.....	51
Figure 27. MS ⁵ of the <i>m/z</i> 1391.5, Man ₄ GlcNAc ₂ LLO from mouse macrophage cell.....	52
Figure 28. MS ⁵ of the <i>m/z</i> 1595.8, Man ₅ GlcNAc ₂ LLO from <i>C. elegans</i>	55
Figure 29. MS ⁴ of the <i>m/z</i> 1595.8, Man ₅ GlcNAc ₂ LLO from <i>C. elegans</i>	56
Figure 30. MS ⁵ of the <i>m/z</i> 1595.8, Man ₃ GlcNAc ₂ LLO from <i>C. elegans</i>	57
Figure 31. MS ⁶ of the <i>m/z</i> 1595.8, Man ₃ GlcNAc ₂ LLO from <i>C. elegans</i>	58
Figure 32. MS ⁵ of the <i>m/z</i> 1595.8, Man ₅ GlcNAc ₂ LLO from mouse macrophage cells.....	59
Figure 33. MS ⁵ of the <i>m/z</i> 1595.8(C-type ion), Man ₅ GlcNAc ₂ LLO from mouse macrophage cells.....	60

Figure 34. MS ⁵ of the <i>m/z</i> 1595.8(Y and B ions), Man ₅ GlcNAc ₂ LLO from mouse Macrophage cells.....	61
Figure. 35. LLO structural isomers isolated for each molecular composition from <i>C.elegans</i>	66
Figure 36. LLO structural isomers isolated for each molecular composition from mouse macrophage cells	67

ABSTRACT

CHARACTERIZATION OF T24D1.4(*ok809*) A PUTATIVE ALPHA-1,2
GLUCOSYLTRANSFERASE IN *C. ELEGANS*

AND

DETAILED STRUCTURAL ANALYSIS OF THE LIPID LINKED
OLIGOSACCHARIDE PATHWAY VIA MS^N

by

William Cobb Wiswall Jr.

University of New Hampshire, December 2009

The formation of glycoconjugates, lipids or proteins covalently linked to carbohydrate groups in biological systems, is a universal process in every form of life studied to date. The carbohydrate moiety of glycoconjugates range in complexity from single monomers to intricately branched structures containing over a dozen residues. This complexity is further compounded by the incorporation of several different monomer types with varying linkage positions and branching patterns. The number of possible carbohydrate structures is astronomical providing significant challenges to characterize, study, and catalog these molecules. Furthermore, assigning biological consequence can be a daunting task considering the numerous interactions caused by the infinite number of biochemical reactions. Methods often focus on one type of glycoconjugate or even a single structure help understand such complexity. The projects described here will attempt to examine the role of the lipid-linked

oligosaccharide (LLO) pathway in the formation of *N*-glycans from a genetic and structural perspective.

CHAPTER 1

GLYCOPROTEIN BIOSYNTHESIS

N-glycosylation, a co-translational protein modification process, is essential and highly conserved in eukaryotic organisms (Huffaker and Robbins 1982). In this process, branched chains of oligosaccharides are covalently linked to polypeptide chains containing the Asn-X-Ser/Thr consensus sequon (Hubbard and Ivatt 1981). A β -*N*-glycosidic bond connects the oligosaccharide chain to the nitrogen atom of the amide group in an asparagine residue of the polypeptide, hence the term *N*-glycan. *N*-glycosylation occurs in four phases beginning on the surface of the endoplasmic reticulum (ER) facing the cytosol; synthesis of the glycan precursor on a dolichol anchor molecule forming a lipid-linked oligosaccharide (LLO); en-bloc transfer of the glycan portion of the LLO to the nascent polypeptide; glycan trimming in ER and Gogi, and monosaccharide elaboration in the medial and trans Golgi (Burda and Aebi 1999).

The resulting *N*-glycan structures have been shown to substantially modulate the intrinsic and extrinsic properties of the glycoprotein potentially altering protein folding, half-life, protein-protein binding, and enzymatic activity (Varki 1993). Unlike DNA replication, RNA translation or protein synthesis, *N*-glycosylation is a non-template driven process constrained by the availability of the appropriate enzymes and substrates. The first phase of *N*-glycosylation is highly conserved in eukaryotes as the mature lipid linked oligosaccharide,

$\text{Glc}_3\text{Man}_9\text{GlcNAc}_2$, is the invariable structure transferred to proteins under ideal conditions. (Lehle, Strahl et al. 2006) However, Golgi processing enzymes were subject to evolution resulting in loose phylogenic associations among higher organisms. Golgi processing alters the mature precursor template to produce a myriad of glycan structures. Therefore, the repertoire of glycan structures produced via the Golgi varies significantly in organisms from different phylogenic groups.

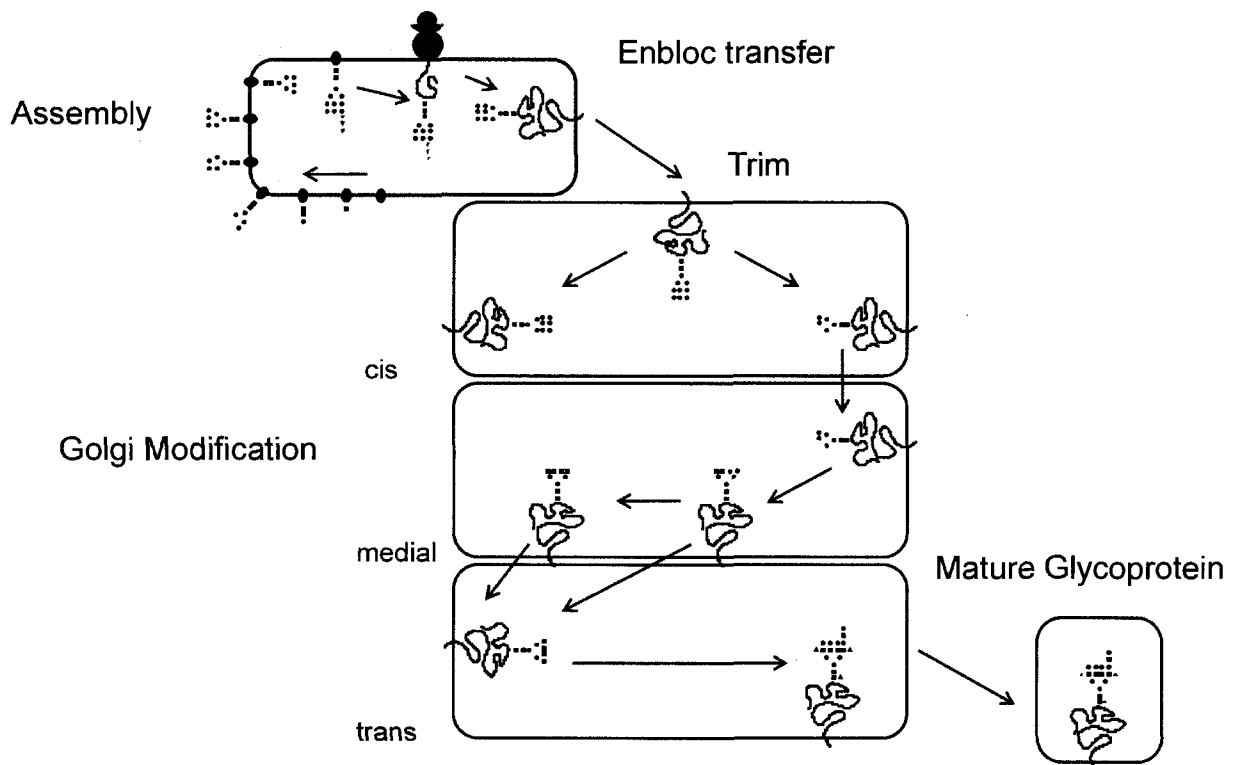


Figure 1. Overview of glycoprotein biosynthesis. *N*-glycosylation, is a co-translation event since the glycan is transferred to the nascent polypeptide as it's threaded through the endoplasmic reticulum. Modification of the mature precursor begins in the ER and continues to the Golgi apparatus.

Resulting *N*-glycans are classified into 3 categories; high-mannose, hybrid and complex, depending upon the level of Golgi processing and monosaccharide elaborations (Kornfeld and Kornfeld 1985). However, all three types contain the conserved trimannosyl core. High mannose glycans are the least modified and contain 5 to 9 mannose residues attached to the core GlcNAc and are formed from ER/Golgi mannosidase activity. Complex type glycans contain GlcNAc residues linked to both branches of the trimannosyl core. These structures can be further elaborated with galactose and sialic acid residues. Hybrid *N*-glycans contain features of both high mannose and complex type as the 1,6 arm consists of mannose residues and the 1-3 is modified with GlcNAc, galactose and sialic acid.

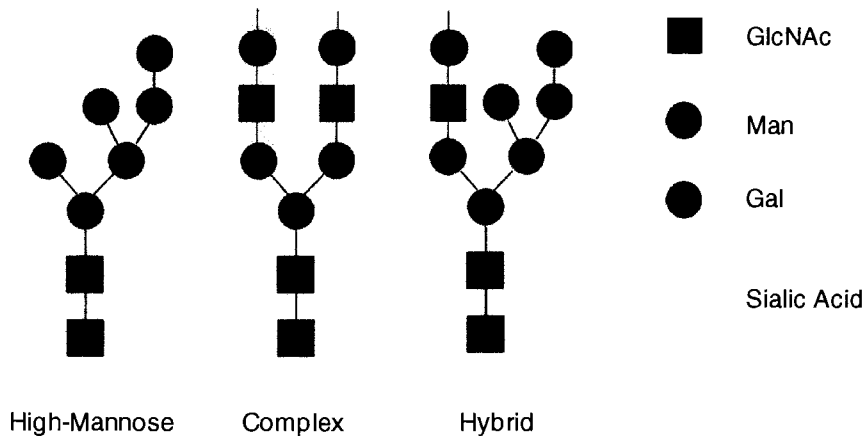


Figure 2. The three types of *N*-glycans

1.1 Biochemistry of the Lipid-Linked Oligosaccharide Pathway

The lipid-linked oligosaccharide pathway is the initial pathway for formation of precursor *N*-glycans (Abeijon and Hirschberg 1992). On the surface of the endoplasmic reticulum facing the cytosol, the lipid anchor molecule dolichol is modified by the addition of specific monosaccharides in a stepwise fashion by the appropriate glycosyltransferases (Unligil and Rini 2000). The first *N*-acetylglucosamine (GlcNAc) residue is added *via* a pyrophosphate linkage to the dolichol backbone from a UDP-GlcNAc donor. The next GlcNAc residue is added by a similar glucosyltransferase albeit through a glycosidic linkage since the monosaccharides are linked sequentially. Three mannose (Man) residues are then added in a branching pattern by the appropriate mannosyltransferases from a UDP-Man donor. Once Man₅ GlcNAc₂-pp-dolichol is complete the entire LLO structure is translocated into the lumen of the ER. This poorly understood process is catalyzed by an ATP-dependent, bi-directional flippase (Hirschberg and Snider 1987). LLO synthesis is continued with the addition of four additional mannose residues. However, the sugar donors in the lumen of the ER are composed of dolichol-linked monosaccharides, which are synthesized on the exterior surface of the ER and transported independently (Burda and Aebi 1999). Finally, glucosyltransferases attach three glucose residues to complete the mature precursor structure Glc₃Man₉GlcNAc₂-pp- dolichol. The glycan portion is

then transferred en-bloc to the growing poly-peptide chain by a multi-subunit enzyme oligosaccharyltransferase (OST) (Knauer and Lehle 1999).

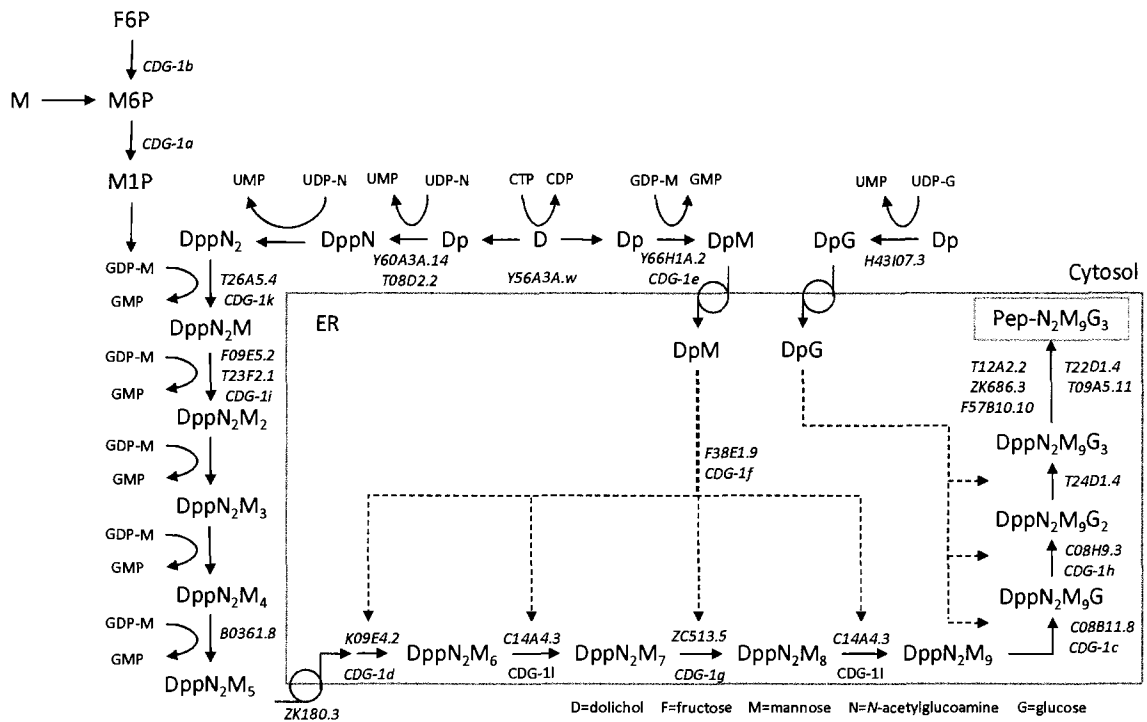


Figure 3. The biochemical reactions of the lipid-linked oligosaccharide pathway (LLO). *C. elegans* gene names are labeled for the appropriate homologues. Identified human CDG-1 genetic mutations are also indicated.

Loss of function in this pathway inhibits the formation of the final LLO precursor which induces hypoglycosylation due to lack of the favored substrate for OST. However, kinetic studies revealed that OST can bind and transfer incomplete LLO glycans at a lower affinity when the mature precursor is structurally deficient (Kelleher and Gilmore 2006). Therefore, truncated LLO precursors are transferred to proteins albeit at a lower rate. In the Golgi apparatus the protein glycans are trimmed down by enzymes and subsequently rebuilt to specificities dictated by local cellular milieu. For this reason, the final

glycan structure is probably minimally affected by defects in the LLO pathway. Instead the major result is the reduction of glycan occupancy (Freeze 2007).

Upon transfer to the nascent polypeptide, alpha-glucosidase binds to the glycoprotein and removes the first glucose residue. Glucosidase II then removes the second glucose residue allowing protein folding chaperones calreticulin and calnexin to bind to the glycoprotein (Ruddock and Molinari 2006). Following protein folding, glucosidase II removes the last glucose residue causing calreticulin and calnexin to disassociate from the glycoprotein. This also signals UDP-glc: glycoprotein glycosyltransferase (UGGT) to bind to the newly folded glycoprotein. This enzyme acts as a sensor and insures proper glycoprotein folding. If the glycoprotein is properly folded it is transported to the Golgi for processing. If however UGGT detects improper folding (probably by hydrophobic interactions) the glycan is reglucosylated allowing the glycoprotein to reenter the calnexin calreticulin cycle. (Parodi 2000). This process continues until proper folding is achieved or the glycoprotein is target for degradation by the ERAD system.

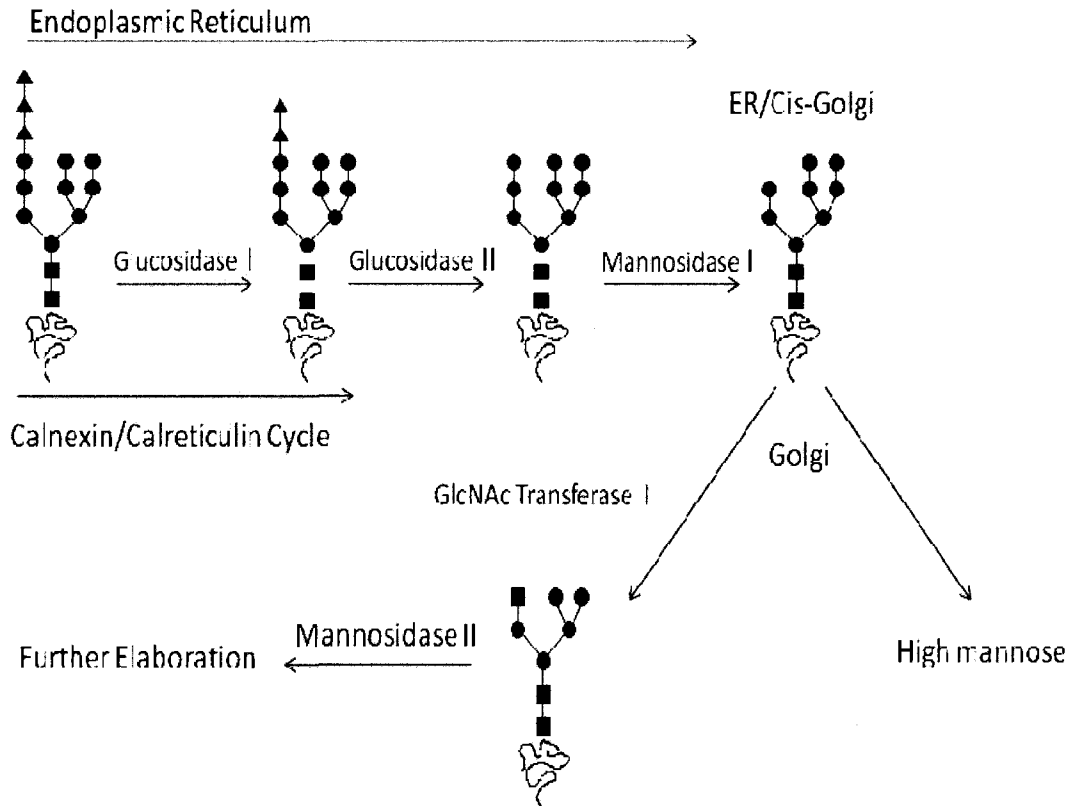


Figure 4. ER and Golgi glycan processing

In a complex biological system, glycan site occupancy, molecular compositions, structural and stereoisomers contribute to a high degree of variability termed microheterogeneity. Different glycan compositions at the same site are identified as glycomers. Many glycoproteins have a range of glycomer structures, e.g., Man₅₋₉ (Rademacher, Parekh et al. 1988). Although, structural variability is a result of Golgi glycosyltransferases, site occupancy must result from oligosaccharyltransferase activity and the calnexin/calreticulin quality control cycle.

CHAPTER 2

CONGENITAL DISORDERS OF GLYCOSYLATION

Congenital Disorders of Glycosylation (CDG) are a group of severe multi-systemic genetically inherited diseases in humans (Jaeken and Matthijs 2001). They are categorized into type I or II depending upon the affected pathway and subtype denoting the specific gene affected. Type I CDGs are caused by defects in the LLO pathway, while types II CDGs are due to glycan processing deficiencies. (Freeze 2001). Classical symptoms include cerebellar hypoplasia, digestive problems, muscle coordination abnormalities, seizures, and failure to thrive. Virtually any system in the body can be affected, which is apparent in the variability of symptoms between types, subtypes and even individuals carrying the same mutation (Jaeken and Carchon 2001). For this reason, diagnosis is only confirmed by isoelectric focusing or genetic analysis. Analysis of LLOs by radio labeling and mass spectrometry has been also employed to a lesser extent and with limited success (Barone, Sturiale et al. 2009).

There are approximately 900 CDG patients worldwide, with the majority suffering from a mutation in the LLO pathway. CDG Ia, the most common of all, results from a mutation in the phosphomannose mutase gene (PPM) which catalyzes mannose-6-phosphate to mannose-1-phosphate (Matthijs, Schollen et al. 2000). The carrier allele frequency for CDG-Ia is as high as 1 in 60 in certain

populations equating into a possible rate of 1/3600 live births. However, only approximately 600 CDG-Ia patients exist worldwide suggesting this disease is misdiagnosed or embryonically lethal in many instances. Indeed, the most commonly mutated allele R141H is not observed in the homozygous state and all CDG-Ia patients carry a compound heterozygous gene, or in other words, each allele contains a different mutation (Schollen, Kjaergaard et al. 2004). Currently only the symptoms of CDG-Ib can be ameliorated by the administration of large amounts of oral mannose. However, the underlying genetic lesion remains and there is no cure or remedy for any other CDG types.

Disorder	Gene	Enzyme	Features
CDG-Ia	PMM2	Phosphomannomutase II	Developmental delay, hypotonia, esotropia, lipodystrophy, cerebellar hypoplasia, stroke-like episodes, seizures
CDG-Ib	PMI	Phosphomannose isomerase	Hepatic fibrosis, protein losing enteropathy, coagulopathy, hypoglycemia
CDG-Ic	ALG6	Glucosyltransferase I Dol-P-Glc: Man ₉ GlcNAc ₂ -PP-Dol Glucosyltransferase	Moderate developmental delay, hypotonia, esotropia, epilepsy
CDG-Id	ALG3	Dol-P-Man: Man ₅ GlcNAc ₂ -PP-Dol Mannosyl-transferase	Profound psychomotor delay, optic atrophy, acquired microcephaly, iris colobomas; hypsarrhythmia
CDG-Ie	DPM 1	Dol-P-Man Synthase I GDP-Man: Dol-P-Mannosyl-transferase	Profound psychomotor delay, severe developmental delay, optic atrophy, acquired microcephaly, epilepsy, hypotonia, mild dysmorphism, coagulopathy
CDG-If	MPDU 1	MPDU1/Lec35	Short stature, ichthyosis, psychomotor retardation, pigmentary retinopathy
CDG-Ig	ALG12	Dol-P-Man: Man ₇ GlcNAc ₂ -PP-Dol Mannosyl-transferase	Hypotonia, facial dysmorphism, psychomotor retardation, acquired microcephaly. Frequent infections

CDG-Ih	ALG8	Glucosyltransferase II Dol-P-Glc: Glc ₁ Man ₉ GlcNAc ₂ -PP-Dol Glucosyltransferase	Hepatomegaly, protein-losing enteropathy, renal failure, hypoalbuminemia, edema, ascites
CDG-li	ALG2	Mannosyltransferase II GDP-Man: Man ₁ GlcNAc ₂ -PP-Dol Mannosyl-transferase	Normal at birth; developmental delay, hypomyelination, intractable seizures, iris colobomas, hepatomegaly, coagulopathy
CDG-lj	DPAGT 1	UDP-GlcNAc: dolichol phosphate N-acetylglucosamine 1-phosphate transferase	Severe developmental delay, hypotonia, seizures, microcephaly, exotropia
CDG-ik	ALG1	Mannosyltransferase I GDP-Man: GlcNAc ₂ -PP-Dol Mannosyl-transferase	Severe psychomotor retardation, hypotonia, acquired microcephaly, intractable seizures, fever, coagulopathy, nephrotic syndrome, early death
CDG-IL	ALG9	Mannosyltransferase Dol-P-Man: Man ₆ and Man ₈ GlcNAc ₂ -PP-Dol Mannosyl-transferase	Severe microcephaly, hypotonia, seizures, hepatomegaly

Table 1. Congenital Disorders of Glycosylation Type I

The etiology of CDG types I and II have been apparent since genetic studies revealed loss of function mutations in genes associated with glycosylation (Marquardt and Freeze 2001). However, understanding the pathologies of these diseases has been quite difficult due to the pleiotropic nature of these genetic lesions. Most, if not all glycoproteins are defective in individuals carrying a homozygous mutation for one of these genes. Subsequently the numerous glycoprotein interactions that cause a specific pathology are almost impossible to isolate, especially in humans. Therefore, use of a genetic model is necessary to circumvent the inherent problems associated with *N*-glycosylation.

2.1 Aberrant *N*-glycosylation and Disease

In addition to CDG types I and II, certain glycan structures have been associated with other disease states such as cancer. Abnormal *N*-glycosylation has been associated with tumor proliferation and metastasis. Specifically, an increase β -1,6 branching and over a expression of sialyl lewis X structures have been preliminary identified as markers in cancer cell lines (Ogata, Ho et al. 1995). More recently, novel *N*-glycan structural isomers have been identified in metastatic brain cells from mouse cancer models (Prien, Huysentruyt et al. 2008). External environmental agents also have the ability to inhibit proper glycan formation. Iso-electric focusing transferrin and α 1-antitrypsin from the serum of alcoholics results in a similar pattern to CDG-I patients (Henry, Froehlich et al. 1999). These examples reveal the dynamic nature of *N*-glycosylation and highlight the importance of proper function in stable biological systems.

CHAPTER 3

USE OF *C. ELEGANS* AS A MODEL ORGANISM

C. elegans has become a fruitful model system for investigating genetic and biochemical aspects of human diseases. Researchers have completely mapped the cell lineage, described its anatomy in detail, and sequenced its genome (Chalfie, Horvitz et al. 1981) (1998). This present knowledge combined with *C. elegans*'s simplistic and short life cycle provides a powerful model system to probe biochemical mechanisms. The animal is extremely tractable to genetic analysis due to the range and power of the robust methods available. Since fundamental processes of development are shared at the molecular level by all animals, *C. elegans* is a suitable analog in which to study profound aspects of human development and disease (Brenner 1974).

Importantly, *N*-glycosylation has been a recent target of study in *C. elegans*. The genome contains homologues to mammalian genes involved in glycan synthesis, processing and modification (Schachter 2004). *C. elegans* was also identified to contain an active homologue of a glycosyltransferase found in humans (Warren, Krizus et al. 2002). Furthermore, RNAi experiments targeting oligosaccharyltransferase caused embryonic and larval lethality suggesting *N*-glycosylation is essential for development in the worm. Subsequent RNAi experiments targeting genes in the *N*-glycosylation assembly pathway revealed detrimental effects in terms of development.

Several groups have investigated the *N*-glycan structures found on glycoproteins in *C. elegans* by mass spectrometry. Although, *C. elegans* does not produce the same repertoire of mammalian glycans, an abundance of high mannose type glycans were identified by all groups. *C. elegans* does not produce sialylated structures found in humans, but instead synthesizes a variety of core fucosylated *N*-glycans (Hanneman, Rosa et al. 2006). Importantly the conserved trimannosyl core is found in *C. elegans* *N*-glycans, suggesting a conserved LLO pathway.

C. elegans is also a useful model for analyzing glycan structural composition as large amounts are easily produced by large scale growth. However, the worm has a thick cuticle that can partially withstand mechanical stress. Although LLO glycans can be isolated from *C. elegans*, mammalian cell culture has proven to be more efficient. Therefore, mouse macrophage cells were also employed for glycan structural analysis.

CHAPTER 4

CHARACTERIZATION OF T24D1.4(OK809)

The LLO pathway has been well characterized in yeast by knock out studies ablating the function of specific glycosyltransferases. Although these studies provided great detail about the enzymatic pathway, they did not provide insight to the role of *N*-glycosylation in metazoan or multi-cellular organisms. This thesis attempts to expand the experimental line of thought learned in yeast to *C. elegans*. *C. elegans* provides a simplistic multicellular animal to investigate the phenotypic consequences of a defective LLO pathway.

4.1 Protein Homology of T24D1.4

Genomic data suggests the existence of *C. elegans* homologues for all LLO glycosyltransferases identified in yeast. Interestingly, none of the *C. elegans* LLO genes have been cloned or characterized. T24D1.4 is a *C. elegans* homologue to the characterized yeast ALG10/DIE2 gene, the last glycosyltransferase in the LLO pathway that catalyzes the formation of the mature precursor Glc₃Man₉GlcNAc₂-pp-dolichol (Burda and Aebi 1998). T24D1.4 is also homologous to the human ALG10/DIE2 gene.

Species	Protein	Description
<i>Caenorhabditis elegans</i>	WP:CE14168 (tag-179)	<i>C. elegans</i> TAG-179 protein; contains similarity to Pfam domain PF04922 DIE2/ALG10 family contains similarity to Interpro domains IPR016900 (Alpha-1, 2 glucosyltransferase Alg10), IPR007006 (Glycosyltransferase, ALG10)
<i>Homo sapiens</i>	(ALG10)	Alpha-1,2-glucosyltransferase ALG10-A
<i>Homo sapiens</i>	(ALG10B)	Putative alpha-1,2-glucosyltransferase ALG10-B
<i>Drosophila melanogaster</i>	FLYBASE:CG32082-PA	
<i>Saccharomyces cerevisiae</i>	SGD YGR227W (DIE2)	Dolichyl-phosphoglucose-dependent alpha-1,2 glucosyltransferase of the ER, functions in the pathway that synthesizes the dolichol-linked oligosaccharide precursor for N-linked protein glycosylation.
<i>Arabidopsis thaliana</i>	SP:Q10254	SubName: Full=Putative uncharacterized protein T1E22_170

Table 2: Wormbase gene homology report. T24D1.4 contain homologous protein sequences to homo sapiens alpha 1,2-glucosyltransferase and yeast ALG10. Reproduced from wormbase.org.

```

Yeast,          125 VPYEFIDEKPHVGGQTLTYLKGKWTQWDPKITTPPGIYILGLI----NYCIKPI
C. elegans,    43 VPEPYMDEIFHITQTRS YCSGNYS-WNPLITTPPALYVISMPLCGGNERYANSI

Yeast,          240 ILQSLSCVLTLPFGPVKSIWLSAFFAGVSCLEFRQTNIIWTGFIMILAVERPAIL
C. elegans,    162 VIWGF-----IGNPIASAFLEFLISILTRQTNIIWAAIYAF-----SVIA

Yeast,          295 LKLFTHAIDDFSNLVLPMKNFVLEFFIYLIWNR-SITLGDKSSH SAGLHIVQIF
C. elegans,    203 LKIIISTA--FS--LWPFITLAIGFAMFIYFNDFQIVLGDAAKHAQPKFHVQPF

Yeast,          354 TVFSLPIWISRNFMKLYKLR IKRKPVQTFEFFIGIMLIIRYFTKVHPPILLADNR
C. elegans,    259 AAHTWTQII PNL LSHLRHLTDMKSLVLQAV----VAVLVVYYSYDHPYLLADNR

Yeast,          419 HYTFYLFRRLLIGN
C. elegans,    320 HFTFYIWRRLFLAN

```

Figure 5. Amino acid sequence comparison of the predicted *C. elegans* T24D1.4 protein to the characterized yeast ALG10 protein. This figure includes regions containing the highest amino acid similarities.

T24D1.4 and ALG10 are orthologs based upon a reciprocal blast test.

The protein sequence of T24D1.4 was blasted to the yeast protein database and

the top match returned was ALG10. The yeast ALG10 protein sequence identified was then blasted against the *C. elegans* protein database which returned only T24D1.4 as the only possible match.

Sequences producing significant alignments	Score	E-Value
YGR227W ALG10/DIE2	183	1.2e-17
YAL037C-B	75	.27
YGL194C-A	54	.84
YGRO36C	64	.96
YMR306W	68	.97

Table 3. Blast results from submitting the T24D1.4 protein sequence against the yeast protein database.

Sequences producing significant alignments	Score	E-Value
T24D1.4	101	8.0e-22

Table 4. Blast results from submitting the yeast ALG10 protein sequence against the *C. elegans* protein database

The Oklahoma Knock-Out Consortium had created a knock out strain deleting the T24D1.4 gene. This strain, (*ok809*), was acquired by the Warren lab since it was the only knock-out of known LLO glycosyltransferases in *C. elegans*. Theoretically, a mutation or knock out in this gene should be the least deleterious since Glc₂Man₉GlcNAc₂-pp-dolichol is formed, a lower affinity substrate for OST. Therefore, this strain would be easier to work with than a mutation that produces severely truncated LLOs that would not be transferred efficiently by OST.

4.2 Specific Aims

The overall goal of this project was to characterize T24D1.4(*ok809*) in a similar manner to the ALG yeast genes. This would provide a genetic model of CDG-I and a non-chemical inhibitor method to study the effects of hypoglycosylation.

In addition to the gene homology, several criteria needed to be addressed to establish T24D1.4(*ok809*) as a model for CDG-I.

- I) *N*-glycosylation should be defective although not absent in the mutant background.
- II) The mature precursor $\text{Glc}_3\text{Man}_9\text{GlcNAc}_2$ should be absent if alpha-1,2 glucosyltransferase activity was null.
- III) The strain should display several phenotypes as hypoglycosylation would affect numerous pathways.

4.3 Materials and Methods

T24D1.4(*ok809*) animals were obtained from the Oklahoma Knock out consortium. Upon arrival they were plated to several large Nematode Growth Media (NGM) plates for cultivation. The strains contained a balancer chromosome because the strain was believed to contain a lethal allele. Once the strain was out crossed 4 times with wild type *C. elegans*, the balancer was

removed and the strain was able to propagate. The knockout was confirmed to be present by PCR. This was accomplished by creating primer sets that could distinguish the difference between the wild type and deletion alleles of *ok809*.

Complementation tests were conducted with *egl-33*, to ensure this was not a previously identified gene. *Egl-33* and T24D1.4(*ok809*) share similar phenotypes, and *egl-33*, although never cloned, was mapped to a position near T24D1.4(*ok809*) (Trent, Tsuing et al. 1983). Complementation analysis revealed that T24D1.4(*ok809*) was not the same gene as *egl-33*.

To address the hypoglycosylation question, we adapted a protein glycoform western blot assay (Cipollo and Trimble 2002). In our experiment, we chose calsequestrin (CSQ-1), an ER localized protein that has been well characterized in *C. elegans*. It is known to have two *N*-glycosylation sites that are occupied 100% of the time (Cho, Oh et al. 2000) (Cho, Ko et al. 2007). By running this protein on a 12% SDS page gel and visualizing the protein on a western blot, different glycoforms can be detected as band shifts, doublets or triplets.

SDS- PAGE gels were made from scratch. The separating gel was made with 6 ml of 30% acrylamide, 3.75 ml of Tris HCL (pH 8.8), 0.15 ml of 10% SDS, 5.1 ml of ddH₂O, 50ul of 10% Ammonium persulfate (APS) and 10 ul of temed. The stacking gel was composed of 1.25mL of 0.5 M Tris HCL (pH 6.7), 0.65 mL of 30 % acrylamide, 3.0 mL of ddH₂O 50 µl of 10% SDS, 22 µl of 10% APS, and 15 µl of temed. The amount of protein loaded from each sample was calculated by a Bradford Assay each time. Sample protein from T24D1.4(*ok809*) and wild

type *C. elegans* was boiled for 4 min with 10 μ l of loading buffer and 4 μ l of β -2 mercaptoethanol. Gels were run at 200V for 90 min. Blot membranes were briefly immersed in MeOH followed by a solution of Tris buffer containing 20% MeOH and 1% SDS. Electro-transfer was completed overnight at 30V in a cold room. The following day, the membrane was washed 3 times with 100% MeOH and left to dry between filter paper. The primary antibody was rabbit anti-CSQ-1, and the working concentration was diluted to 1:5000. The secondary antibody, conjugated horse radish peroxidase, was acquired from sigma and diluted 1:50000.

Next the LLO precursors were analyzed via MALDI-TOF CFR. Batches of wild type and T24D1.4(*ok809*) *C. elegans* were grown on large trays containing NGM seeded with RR1 *E. coli* bacteria. Synchronized L1 were allowed to propagate for approximately 6 days. Upon clearing of the bacteria, the *C. elegans* were washed off the plates and cleaned by sucrose flotation. Harvested animals were placed into a 30% sucrose solution and centrifuged at 160g. In this method, only live animals float to the surface while dead animals and debris collect on the bottom. Live worms are pipetted off to a fresh tube containing 100% dH₂O. Following three dH₂O washes to remove any excess sucrose, the animals were flash frozen and stored at -80°C.

The LLO extraction protocol was adapted from experiments involving HPLC for analysis (Grubenmann, Frank et al. 2004). Worm pellets were subjected to disruption with a polytron or Barocycler (Pressure Biosystems, South Easton, MA). *C. elegans* pellets of approximately 1.5g were dried down to

remove excess water prior to LLO extraction. The pellets were then extracted twice with 2:1 chloroform:methanol and the aqueous layer was discarded. The remaining pellets were next extracted twice with 10:10:3 chloroform: methanol: water. The aqueous layer was removed and dried under nitrogen gas flow. The dried extract was then incubated in 0.2 M HCL in 50% isopropanol for 1hr. This hydrolyzes the pyrophosphate bond freeing the glycan from the dolichol backbone. The sample was dried again under nitrogen gas flow to remove the solvent and acid. The dried extract was then dissolved in 2% acetonitrile (AcCN) and checked for acidity with pH strips. Two reverse-phase columns were prepared. First a C18 which was washed with 5ml of MeOH, 5ml of AcCN, 5ml of 3:1 AcCN, and 6ml of 2% AcCN. The sample was then applied to the column and allowed to flow through by gravity. The flow through was collected and the column was washed with 3ml of 2% AcCN. The second was a porous graphitized carbon (PGC) which was prepared for the next column. The sample was then applied to the PGC column and washed with 6ml of 2% AcCN. The glycans were eluted with 5 ml of 3:1 AcCN: H₂O. Finally the sample was dried in a SpeedVac (Savant, Holbrook, NY). The samples were then spotted onto a MALDI-TOF target plate with 10mg/ml of DHB in 50% AcCN. Spectra were acquired in the positive mode using a MALDI-TOF CRF (Kratos-Shimadzu Analytical, Manchester,UK) .

4.4 Results

4.4.1 Calsequestrin Hypoglycosylation Blot

CSQ-1 in a wild type background has been shown to be synthesized with two *N*-linked glycan chains. This was confirmed and visualized in this study as one band at the expected molecular weight of 64kD. Treatment with endo-H caused the wild type band to migrate further, suggesting the removal of two glycan chains. In the T24D1.4(*ok809*) background, CSQ-1 was visualized as two distinct bands, possibly indicating the presence of two glycoforms. Treatment with endo H collapsed the two bands into one, supporting the idea of two glycoforms present on CSQ-1 from the T24D1.4(*ok809*) background.

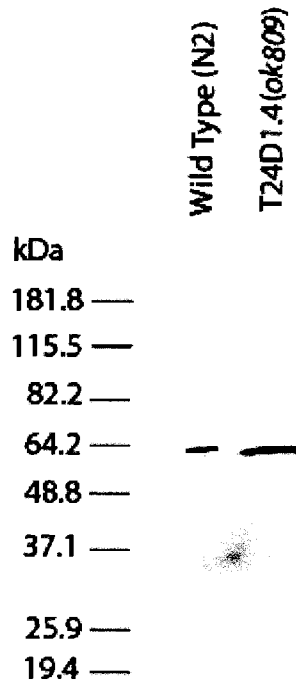


Figure 6. Calsequestrin western blot from wild type and T24D1.4(*ok809*) protein preparation. This blot was completed as a test run for the CSQ antibody. The T24D1.4(*ok809*) band appeared to migrate further than the wild type counterpart.

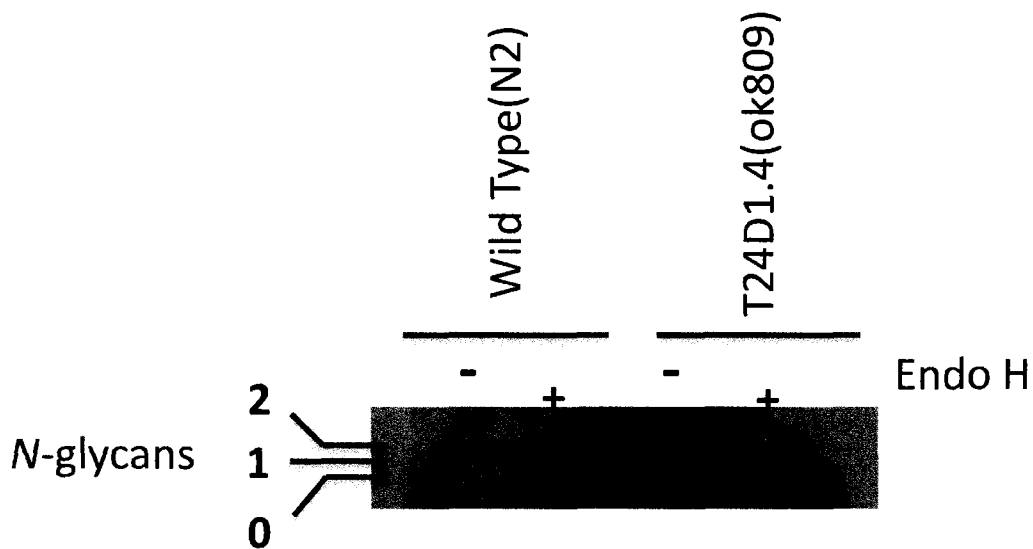


Figure 7. Calsequestrin western blot with and without endo-H treatment. Although the background noise is significant, the T24D1.4(*ok809*) CSQ-1 migrated as two distinct bands. Endo-H treatment of the T24D1.4(*ok809*) protein caused CSQ-1 to migrate as one band.

4.4.2 MALDI -TOF CFR of LLO Precursor Glycans

Spectra acquired from the wild type *C. elegans* sample on the MALDI-TOF CFR revealed peaks consistent with molecular weights of LLO precursors. Peaks representing $\text{Man}_5\text{GlcNAc}_2$ through $\text{Glc}_3\text{Man}_9\text{GlcNAc}_2$ were observable.

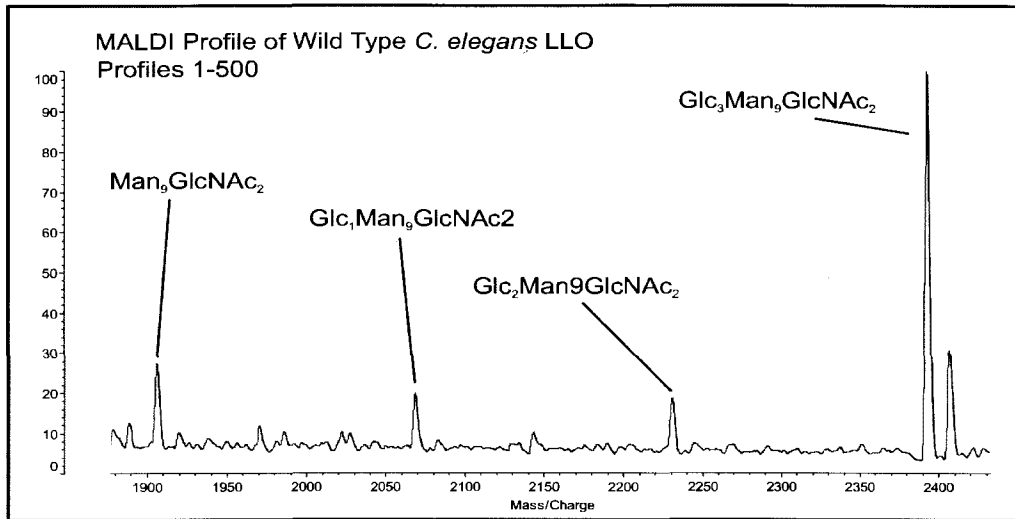


Figure 8. MALDI-TOF Profile of Wild Type *C. elegans* LLOs

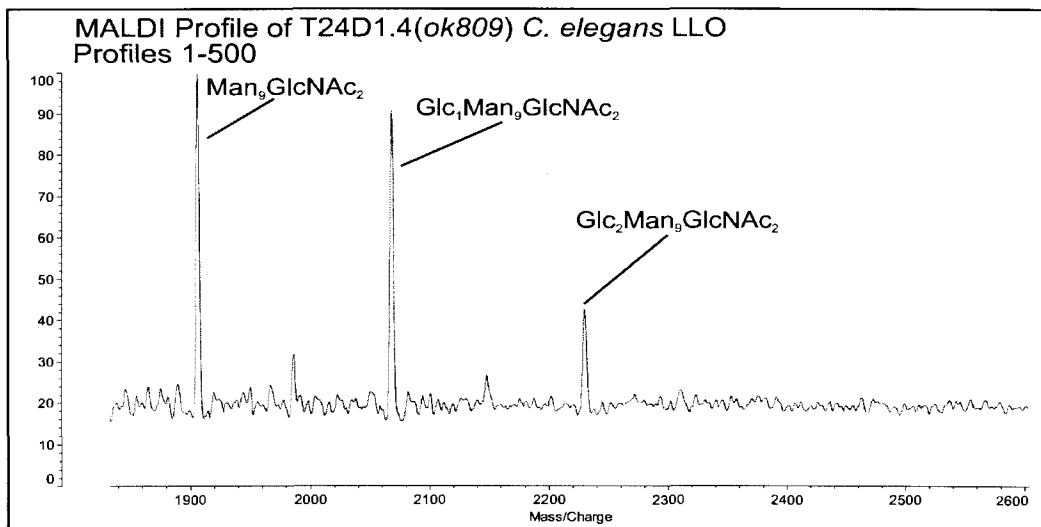


Figure 9. MALDI-TOF Profile of T24D1.4(*ok809*) *C. elegans* LLO

Results for T24D1.4(*ok809*) were similar in that $\text{Man}_5\text{GlcNAc}_2$ through $\text{Glc}_2\text{Man}_5\text{GlcNAc}_2$ could be identified. However, the mature precursor $\text{Glc}_3\text{Man}_5\text{GlcNAc}_2$ was not detectable. This was consistent with the hypoglycosylation blot and expected results inferred from gene homology with ALG10.

4.4.3 Phenotypic Analysis

Although *C. elegans* hermaphrodites contain only 959 cells, a trained person can easily recognize many different phenotypes. They are easily employed as markers for genetic crosses and distinct phenotypes can also provide insight into the biology behind the genetic mutation. Since T24D1.4(*ok809*) had several conspicuous phenotypes, the appropriate assays were performed to quantitatively analyze them for comparison.

The first phenotypic analysis quantitatively confirmed a brood size deficiency for the T24D1.4(*ok809*) strain. The data indicates that the mutant knockout strain produces a lower amount of viable progeny compared to the wild type counterpart at optimal growing conditions of 20°C. Wild type *C. elegans* typically lays approximately 280 eggs per brood, while the T24D1.4(*ok809*) strain lays 90 eggs per brood on average.

In addition, T24D1.4(*ok809*) appears to be a temperature sensitive mutant as the number of viable progeny decreases at 25°C. It was noted that a large proportion of mutant embryos did not reach the first larval stage.

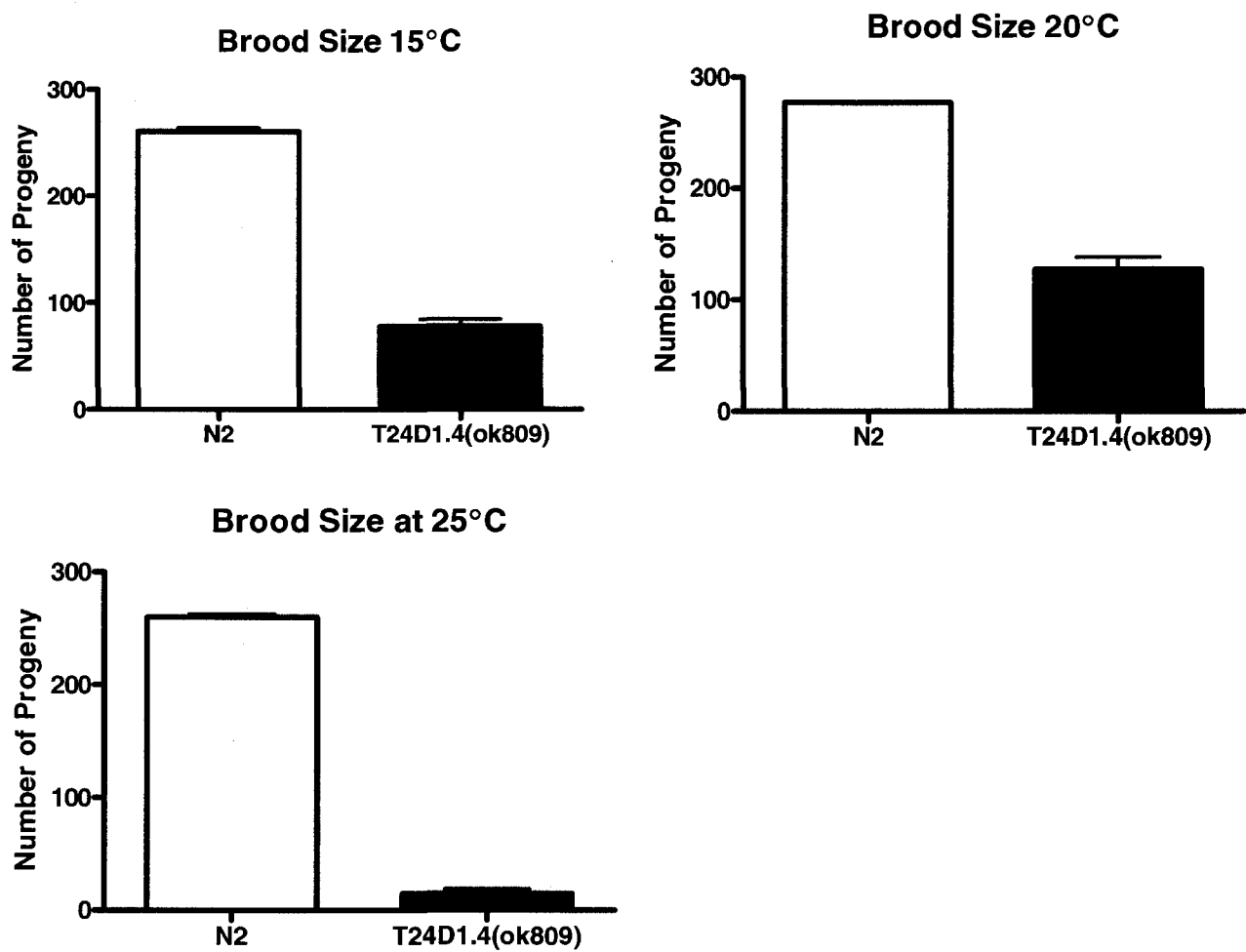


Figure 10. *C. elegans* brood sizes at 15°C, 20°C and 25°C, wild type (N2) compared to T24D1.4(ok809)

The obvious brood size insufficiency suggested an embryonically lethal phenotype combined with an egg laying defect. To investigate this phenotype, T24D1.4(ok809) was assayed for sensitivity to serotonin and imipramine which normally induces egg laying in wild type *C. elegans*. This assay indicated that T24D1.4(ok809) share a phenotype close to the egl-A class of animals

categorized by Trent and Horvitz. Serotonin and Imipramine did not induce egg laying in T24D1.4(*ok809*) animals.

		Serotonin				
eggs laid		>=8	>=4	>=1	>=0	
		+	(+)	(-)	-	total n/%
N2	WW	66	13	2	1	72
		78%	18%	3%	1%	100%
	(Trent & Horvitz)	338	65	22	25	440
		77%	13%	5%	6%	100%
T24D1.4(<i>ok809</i>)	WW	0	6	15	51	70
		0%	9%	19%	73%	100%
Egl-A	(Trent & Horvitz)	4	8	16	219	247
		2%	3%	6%	89%	100%
		Imipramine				
eggs laid		>=8	>=4	>=1	>=0	
		+	(+)	(-)	-	total n/%
N2	WW	66	5	1	0	72
		92%	7%	1%	0%	100%
	(Trent & Horvitz)	356	51	15	5	427
		83%	12%	4%	1%	100%
T24D1.4(<i>ok809</i>)	WW	0	6	20	45	71
		0%	8%	28%	63%	100%
Egl-A	(Trent & Horvitz)	5	12	24	189	230
		2%	5%	10%	82%	100%

Table 5. Egg laying deficiency assay.

In addition to the obvious brood size deficiency, T24D1.4(*ok809*) animals grew extremely slowly. Furthermore, generation time was significantly desynchronized compared to wild type animals that generally reach the reproductive stage at approximately 70 hours.

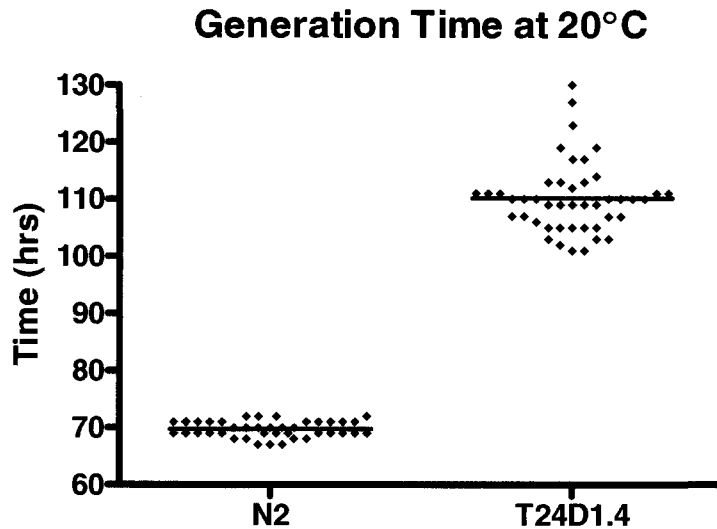


Figure 11. Generation time of T24D1.4(*ok809*) compared to wild type(N2) *C. elegans*.

T24D1.4(*ok809*) animals were tested for sensitivity to tunicamycin, a potent inhibitor of *N*-glycosylation. Tunicamycin prevents the transfer of the first GlcNAc to the lipid carrier dolichol phosphate, essentially inhibiting the first step of the LLO pathway. (Tkacz and Lampen 1975). At 3µg/ml of tunicamycin wild type *C. elegans* displays multiple phenotypes expected from defective glycosylation. Doses above 3µg/ml cause a high percent of larval lethality in wild type animals. 100% lethality is observed at between 5µg/ml and 10µg/ml. T24D1.4(*ok809*) animals display a high sensitivity to low doses of tunicamycin. Effects are observed at only 0.02µg/ml of tunicamycin. Doses at or above 0.16µg/ml cause 100% larval lethality in T24D1.4(*ok809*) animals.

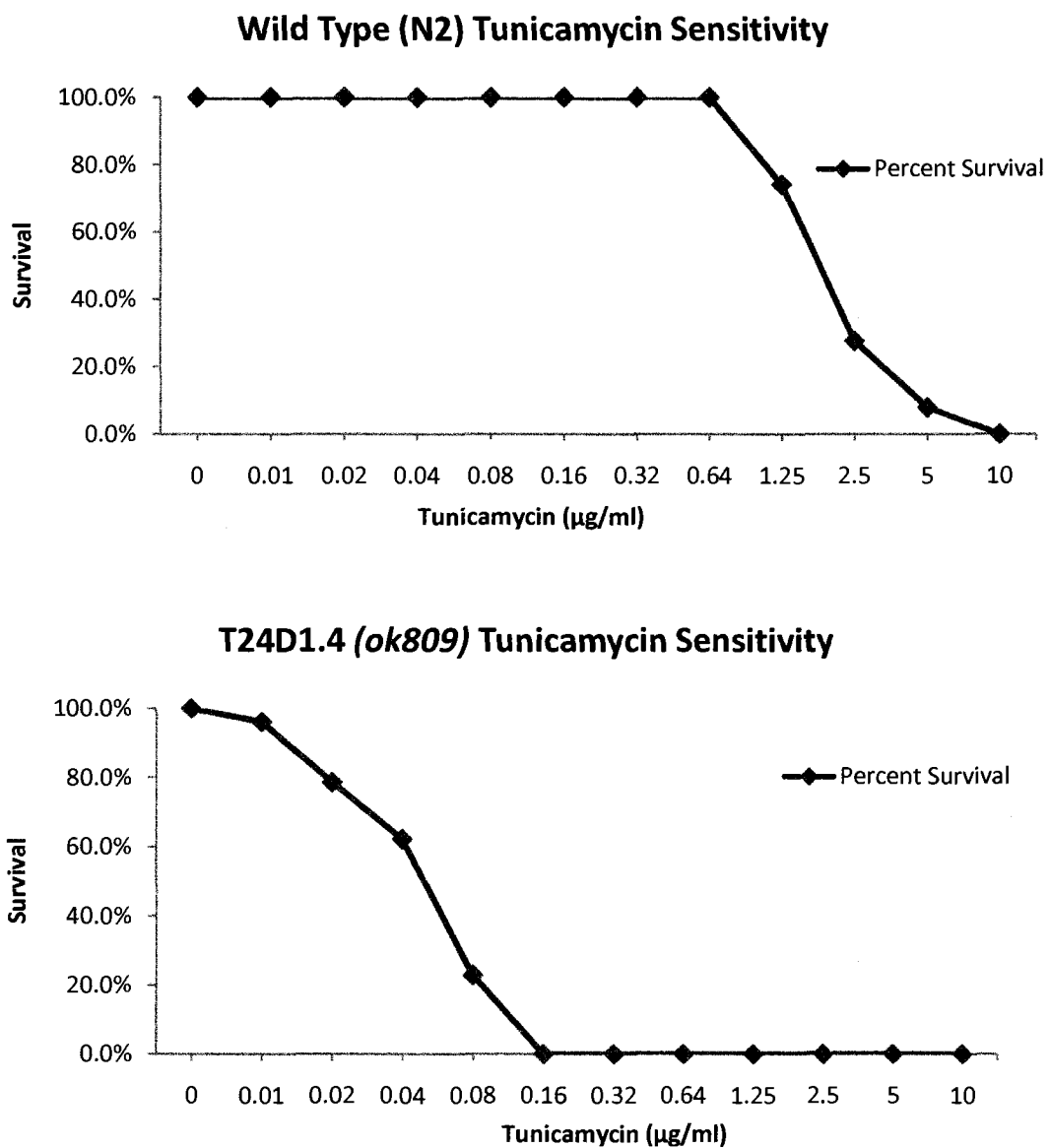


Figure 12. Tunicamycin sensitivity assay. Wild type (N2) *C. elegans* compared to T24D1.4

4.5 Conclusions

Experiments completed in this project support the hypothesis that T24D1.4 is the *C. elegans* homologue of the yeast ALG10 gene. The hypoglycosylation blot clearly showed that the CSQ-1 protein migrates as two distinct bands in the T24D1.4(*ok809*) strain. This was even more evident when examining the blot photo on a light box. When treated with endo-H the T24D1.4(*ok809*) band migrates as one band at a lower molecular weight. In addition, the endo-H treated T24D.1(*ok809*) band migrates at a similar molecular weight as the wild type control treated with endo-H. This change in migration when treated with endo-H can be attributed to a loss of *N*-glycan chains. Therefore, the CSQ-1 doublet observed from T24D1.4(*ok809*) is most likely produced from different amounts of glycan chains. This suggested that T24D1.4(*ok809*) produces CSQ-1 as different two different glycoforms. This result is comparable to the ALG experiments examining protein hypoglycosylation.

The MALDI-TOF analysis revealed the expected LLO compositions in the wild type control. The T24D1.4(*ok809*) profile contained many of the expected LLO compositions with the important exception of the mature precursor. This peak should appear at a *m/z* of 2392. $\text{Man}_5\text{GlcNAc}_2$ through $\text{Glc}_2\text{Man}_9\text{GlcNAc}_2$ were clearly identifiable in this sample. The lack of the $\text{Glc}_3\text{Man}_9\text{GlcNAc}_2$ is a negative result which can be problematic for providing a definitive answer. However, this result is in agreement with the hypoglycosylation blot and genomic

data. It is likely that T24D1.4(*ok809*) does not produce the mature LLO precursor.

Phenotypic analysis revealed multiple defects in terms of development indicating a pleiotropic effect as expected. From simple observation using a light microscope T24D1.4(*ok809*) animals carries the following phenotypes; dumpy (short, or football shaped), uncoordinated (does not travel in a normal sinusoidal movement), growth impaired, (generation time is longer the 3 days), and embryonic lethal (noticeable amount of eggs do not hatch to the first larval stage). T24D1.4(*ok809*) animals were hypersensitive to low doses of tunicamycin, displaying effects at 0.02µg/ml.

The brood size assay indicated that T24D1.4(*ok809*) animals laid approximately 80-90 eggs per brood, which is well under the expect wild type size of 280. This phenotype was exacerbated when the animals were grown at 25°C, resulting in only approximately 15-20 viable animals per brood.

T24D1.4(*ok809*) animals were not sensitive to imipramine or serotonin. These neural transmitters induce egg laying in wild type animals. T24D1.4(*ok809*) was similar to *egl-A* class of egg laying defective mutants classified by the Horvitz lab which are associated with improper vulva function or the vulval and uterine muscles (Trent, Tsuing et al. 1983). The etiology of the egg laying defect in T24D1.4(*ok809*) could also be caused by neuronal defects, however, this would require further investigation.

Hypersensitivity to tunicamycin could also indicate a deficient glycosylation pathway in T24D1.4(*ok809*) animals. This could be inferred as an

additional perturbation to the LLO pathway resulting in severe (larval lethality) phenotypic effects.

4.6 Future Work

Overall, T24D1.4(*ok809*) meets all of the previously determined criteria to classify this mutant as a alpha 1,2 glycosyltransferase. This strain may be used in place of glycosylation chemical inhibitors to study the physiologic effects of hypoglycosylation. Future work could include genome wide screen for suppressor genes or synthetic lethal genes. The easiest method to screen for these genes would involve a RNAi screen. The T24D1.4(*ok809*) strain would be crossed with the *rrf-3* strain to create a double mutant sensitive to RNAi. Individual RNAi constructs could be fed to the strain via bacterial lines. Originally, candidate genes identified from the RNAi screen performed in the Warren Lab were to be further investigative by this method.

Phenotypic assays provide a method to identify specific pathologies caused by hypoglycosylation and targets for future investigation. Several assays indicate a severe egg laying defect, a potential target for investigate the role of *N*-glycosylation in development. For example, neuronal migration could be studied in correlation with GFP studies of T24D1.4. In general, it would be interesting to examine the temporal and cellular location of the gene expression of T24D1.4. This could determine the activity of glycosylation in terms of development.

CHAPTER 5

COMPARATIVE STRUCTURAL ANALYSIS OF LIPID LINKED OLIGOSACCHARIDES IN *C. ELEGANS* AND MOUSE MACROPHAGE CELLS

The advent of sequential mass spectrometry (MS^n) with ion trap analyzers has identified numerous glycan structural isomers on a small subset of glycoproteins. Biological significance has also been implied by the characterization of unique glycan isomers associated with metastatic brain tumors in mouse models. (Prien, Huysentruyt et al. 2008). MS^n provides paramount sensitivity and comprehensive glycan structural information while utilizing small sample amounts. These characteristics provide an inclusive platform to study the transient molecules of the LLO pathway.

The objective of this project was to perform a comparative analysis of LLO structural isomers found in *C. elegans* and mammalian cells. The discovery of unique glycan isomers on proteins questions the specificity of entire glycosylation pathway and presents the challenge to identify the source of these isomers (Prien, Ashline et al. 2009). However, the presence of LLO structural isomers does not infer a direct link to ones found on proteins. Multiple exoglycosidases in the ER and Golgi are able to trim down the $Glc_3Man_9GlcNAc_2$ structure. Since glycans are extensively modified in the Golgi, the $Glc_3Man_9GlcNAc_2$ structure is only transiently present on the glycoprotein. Therefore, *N*-glycan isomers found on proteins are most likely a result of Golgi processing. Furthermore, some studies suggest that LLO intermediates

extracted and isolated from cells may be an artifact of the process itself. This theory explains that upon cell lysis LLOs normally contained to the ER *in vivo* are exposed to degradation enzymes. However, our study shown here and experiments performed by the Lehrman group suggest this process only minimally effects the glycan structure of the LLOs (Gao and Lehrman 2002).

The Golgi glycan processing pathway suggests that there would be no reason to catalogue specific isomers in the LLO pathway since these structures would be invariably discarded. However, identifying the exact glycan isomers created in this pathway could potentially be useful for disease markers. In addition, current literature presents definitive detailed structures based upon methods incapable of distinguishing structural isomers (Kelleher, Karaoglu et al. 2001). Therefore, this method at the very least will provide additional insight to the nature of this pathway. Furthermore, this method could be easily employed to provide an addition method for CDG diagnosis without going past MS¹ analysis.

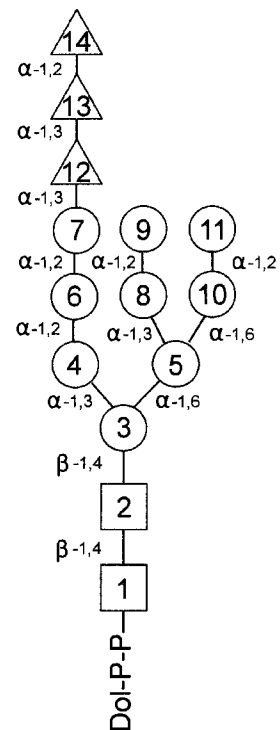


Figure 13. The expected structure for the mature LLO. Current theory definitively uses this linkage and construction order.

5.1 Sequential Mass Spectrometry

As an analytical tool, mass spectrometry has been a powerful technique employed for the detection and characterization of biopolymers. The diverse applications offered by mass spectrometry combined with its inimitable sensitivity provide a reliable method to uncover structural details of complex carbohydrates. Specifically, sequential mass spectrometry (MS^n) with ion-trap analyzers has allowed for unprecedented detection and analysis of carbohydrates. (Ashline, Singh et al. 2005).

By preparing glycan samples as methyl derivatives, ion-trap mass spectrometry (ITMS) provides an effective method for uncovering carbohydrate structural detail and isomers in biological samples. This is based upon the ability to disassemble parent ions and separate the resulting fragment ions in the gas-phase for subsequent fragmentation. Furthermore, the fragmentation pathways are reproducible so that spectra data represents the structure of the parent ion (Ashline, Lapadula et al. 2007). Although glycan structural isomers have the same molecular composition, they fragment through different pathways in the gas-phase. Therefore, this method allows for structural elucidation without additional separation techniques.

Permethylation of the carbohydrate analyte is an essential prerequisite for purification and subsequent MS^n analysis. Permethylation transforms hydroxyls to methyl ethers (Ciucanu and Kerek 1984). This changes the normally hydrophobic carbohydrate to a lipophilic derivative and allows for extractions in

non-polar solvents. Even more important, blocking hydroxyls with methyl groups allows for the identification of carbohydrate topology since CID fragmentation results in hydroxyl scars. These scars are identifiable through mass spectrometry since the loss of a methyl group is reflected by a loss in mass.

ITMS combined with permethylation can also provide in depth structural information through fragmentation of smaller oligosaccharides. Fragmentation of disaccharides and trisaccharides produces cross ring cleavages through a retro Diels- Alder reaction. The resulting spectra provides diagnostic ions that reflect linkage, branching detail and even anomericity configurations.

Previously, investigations in the LLO pathway employed enzymology, HPLC coupled with radiolabeling , or fluorophore-assisted carbohydrate electrophoresis (Lehrman and Gao 2003) (Frank and Aebi 2005). Although these techniques are valuable in identifying the components of the LLO pathway in comparison between molecular compositions, they fail to discern structural isomers. This project extends ion-trap applications to the lipid linked oligosaccharide pathway.

5.2 Materials and Methods

Several grams of *C. elegans* were harvested by large scale growth for LLO glycan structural analysis. The protocol was followed as described previously in chapter 4 with alterations stated here. Dialysis of sample

preparations was completed after cell lysis or *C. elegans* cuticle disruptions. This was incorporated into the procedure to move any free glycans. Dialysis cassettes with a molecular weight cutoff of 2KDa were used. Dialysis was performed for 3 hours in 20mM ammonium bicarbonate (NH_4CO_3), 0.05% and sodium dodecyl sulfate (SDS) at 4°C. This was followed by an overnight dialysis in 10mM NH_4CO_3 and 0.02% SDS. Extractions and column purification were performed as described in chapter 4. Following PCG cleanup, the samples were dried down in a SpeedVac (Holbrook, NY) and reduced by the addition of 200 μl of 10mg/ml NaBH_4 in 0.1M NaOH. After an overnight incubation at room temp the reaction was stopped by the addition of three drops of glacial acetic acid and dried down again in a SpeedVac (Holbrook, NY). The following additions were then added and evaporated consecutively under nitrogen to remove borate esters; 3mls of methanol, 3 ml of 1% acetic acid in methanol, followed by 3 ml of toluene repeated twice. To remove the salts, the reduced LLO samples were run on DOWEX AG50 W X8-400 cation-exchange resin (Sigma-Aldrich, St. Louis, MO). The column was washed with 2 ml of HPLC H_2O . The flow-through was collected and dried in the SpeedVac (Holbrook, NY). Samples were then permethylated by the following procedure. 1ml of DMSO and 100 μl of iodomethane were added to both samples with crushed sodium hydroxide. Samples were vortexed at room temp for 1hr. The reaction was stopped by the addition of 1mL of HPLC H_2O while the samples were on ice. This was followed by the addition of 1mL of dichloromethane. The samples were vortexed and the bottom organic layer was removed and saved in a new tube. This processed

was repeated three times. The removed organic layer was then washed with 1 ml of HPLC H₂O. This was repeated six times, saving the top organic layer each time. The sample was then dried down under nitrogen and lyophilized overnight.

Samples were analyzed on a LTQ mass spectrometer (ThermoFinnigan, San Jose, CA) equipped with a TriVersa Nanomate (Advion, Ithaca, NY) for sample infusions. Collision energy was set to 35%. Activation Q was set to 0.25. Scans were acquired in the positive mode.

Testing for *in vivo* glycan degradation was accomplished by incubating standard Glc₃Man₃ with mouse macrophage cell lysates for 6 hours at room temp. Following incubation the LLOs were isolated as previously described.

5.3 Results

5.3.1 LLOs are not substantially Degraded Upon Cell Lysis

Personal communication with the Gilmore lab suggested that LLO isomers identified by MSⁿ could be an artifact of cell lysis. In order to test this hypothesis Glc₃Man₉ standard were incubated with cell lysates from mouse macrophage cells. The LLOs were subsequently re-purified and analyzed by MALDI-TOF-CFR. The results indicated that the Glc₃Man₉ standard was not degraded as the major peak of *m/z* 1907.9 was still present. Compared to the pure standard, the spectra from the incubated LLOs contained higher background noise and peaks probably corresponding to contaminants.

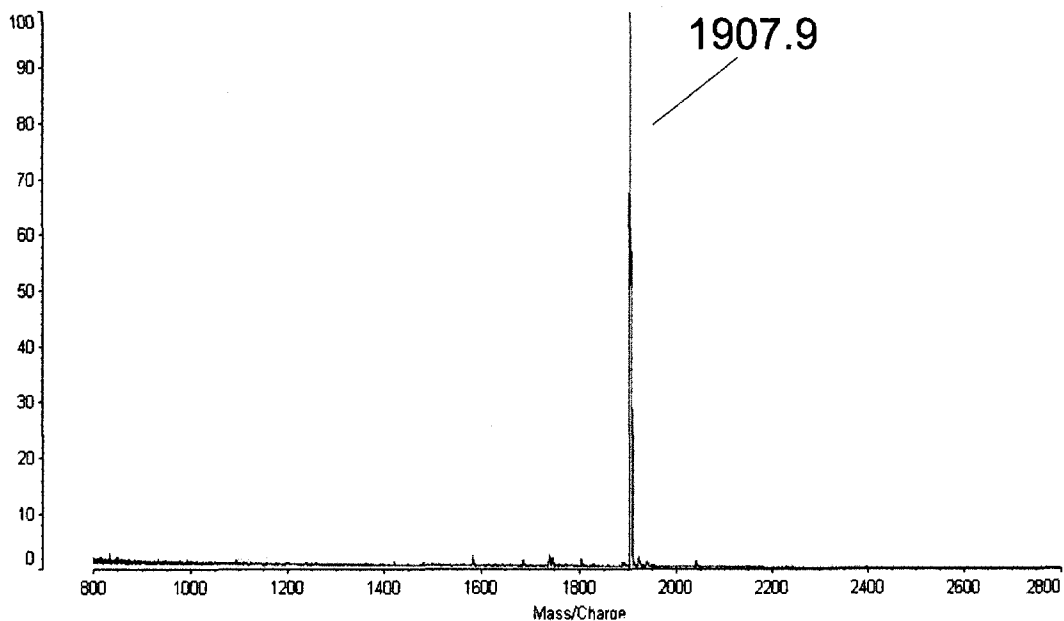


Figure 14. MALDI-TOF-CFR profile of a pure Glc_3Man_9 standard. Profiles 1-1000.

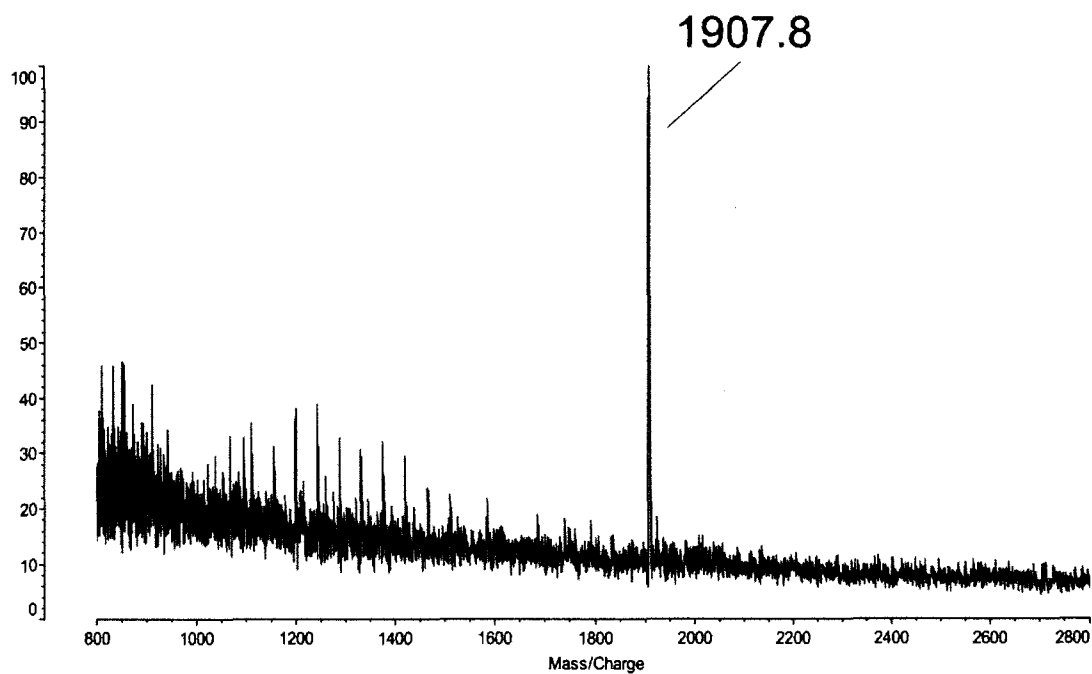


Figure 15. MALDI-TOF-CFR profile of Glc_3Man_9 standard re-purified after an 8 hr incubation in fresh mouse macrophage cell lysate. Other peaks present did not correspond to any possible glycan degradation products from Glc_3Man_9 . Profiles 1-1000

5.3.2 Comparative Structural Analysis Man₃GlcNAc₂LLO

Analysis of the conserved tri-mannosyl core revealed an isomeric mixture of two structures in *C. elegans*. The expected structure containing α 1,6 and α 1,3 linkages at the first mannose residue was determined by the following pathway: m/z 1187.6 \rightarrow m/z 894.3 \rightarrow m/z 737.3 \rightarrow m/z 519.2. The MS⁵ spectra revealed the diagnostic m/z 431 (^{3,5} A-ion) suggesting the presence of an α 1,3 linkage. The m/z 401 (^{2,4} A-ion) suggests an α 1,6 linkage.

Alternatively, a linear core structure is observed in the following fragmentation pathway: m/z 1187 \rightarrow m/z 894 \rightarrow m/z 667. MS⁴ spectra of this C-ion produced an m/z 472 fragment only consistent with an internal mannose with only one open hydroxyl group. Normally, the branching mannose contains two open hydroxyl groups corresponding to a peak of m/z 458. This peak was also observed indicating a mixture of a branching and linear structure.

Analysis of Man₃GlcNAc₂ in mouse macrophage cells also revealed the expected core branching structure containing α 1,6 and α 1,3 linkages. Again, MS⁴ of the m/z 667(C-ion) produced an m/z 472 peak indicating a linear core structure.

The mouse macrophage contained an unusual terminal HexNAc structure. This was apparent from the m/z 928(Y-ion) observed from MS² fragmentation of the m/z 1187.6. This can only be explained by the loss of a terminal HexNAc. In addition, this would indicate the presence of only 1 HexNAc at the core.

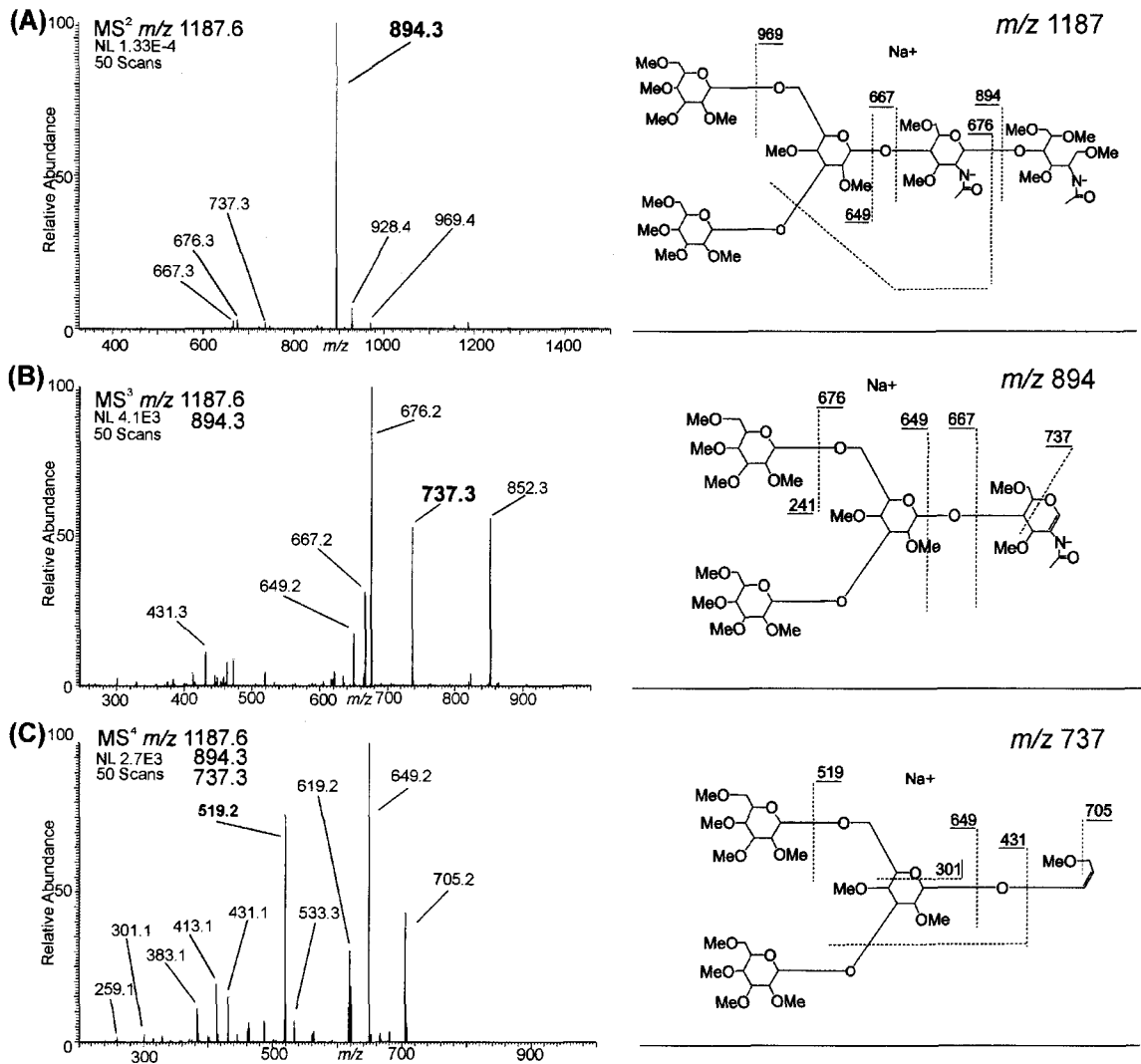


Figure 16. MS⁴ pathway of the m/z 1187.6, Man₃GlcNAc₂ LLO from *C. elegans*.

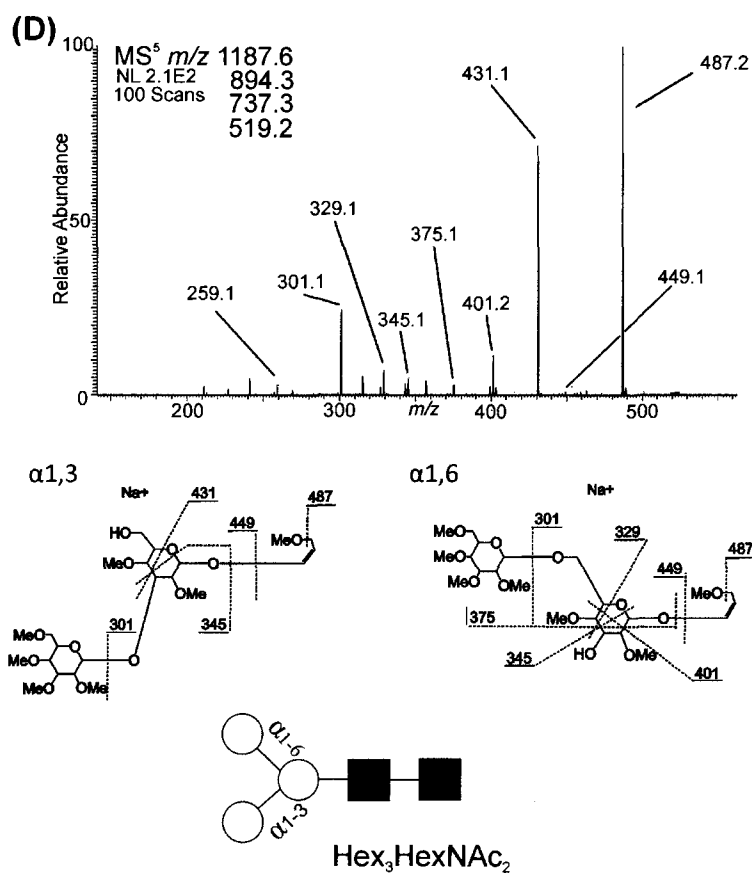


Figure 17. MS⁵ spectra of 1187.6 m/z , Man₃GlcNAc₂ LLO from *C. elegans* and fragmentation assignment for the m/z 519 ion. The cross ring cleavages produce diagnostic ions of m/z 329, m/z 375, and m/z 401, m/z 431 indicating a mixture of $\alpha 1,6$ and $\alpha 1,3$ linkages at the core. This structure is the expected glycan precursor Man₃GlcNAc₂.

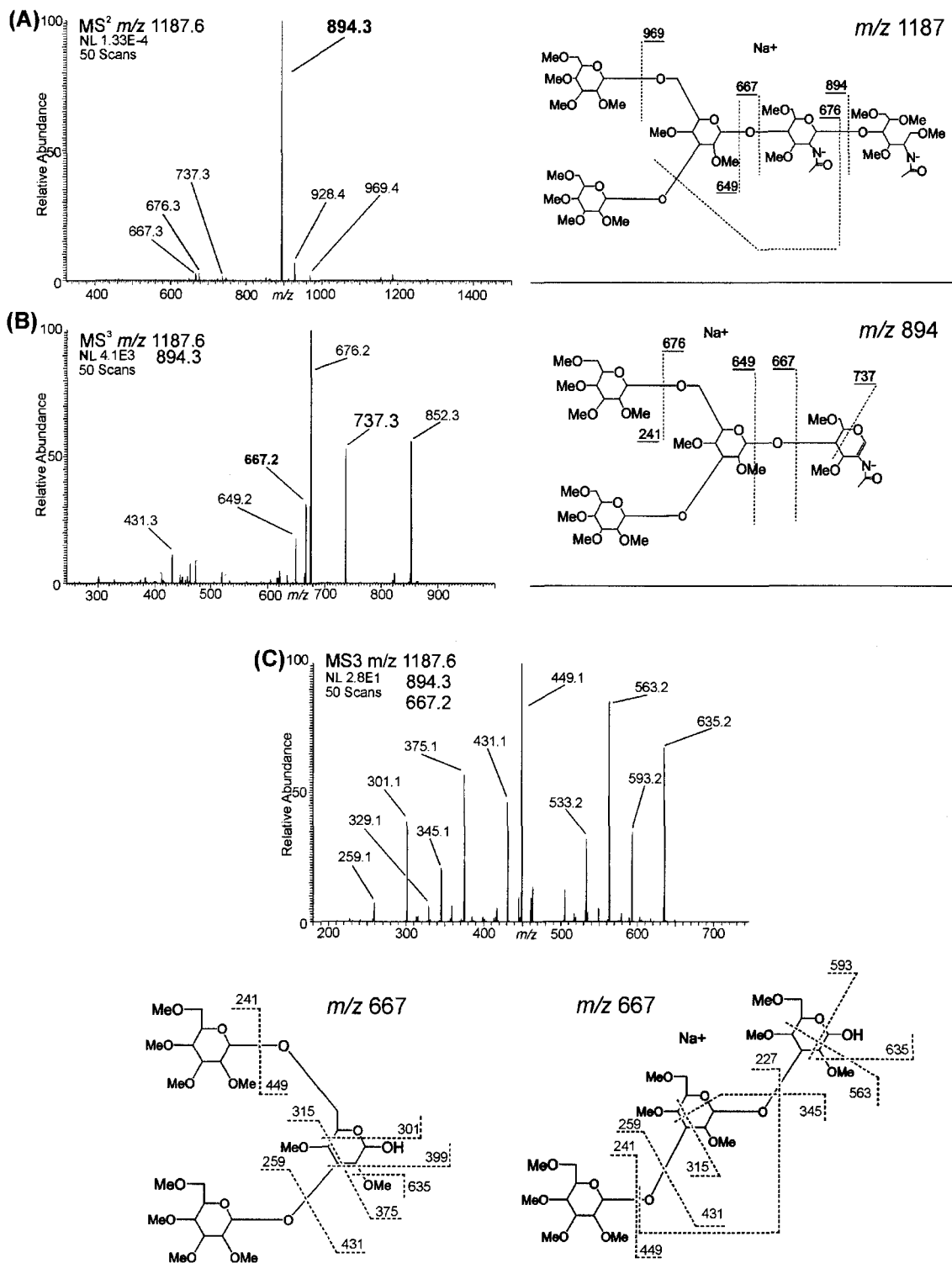


Figure 18. MS⁴ spectra of m/z 1187.6, Man₃GlcNAc₂ LLO from *C. elegans* and ion fragmentation assignment of the m/z 667 C-type ion.

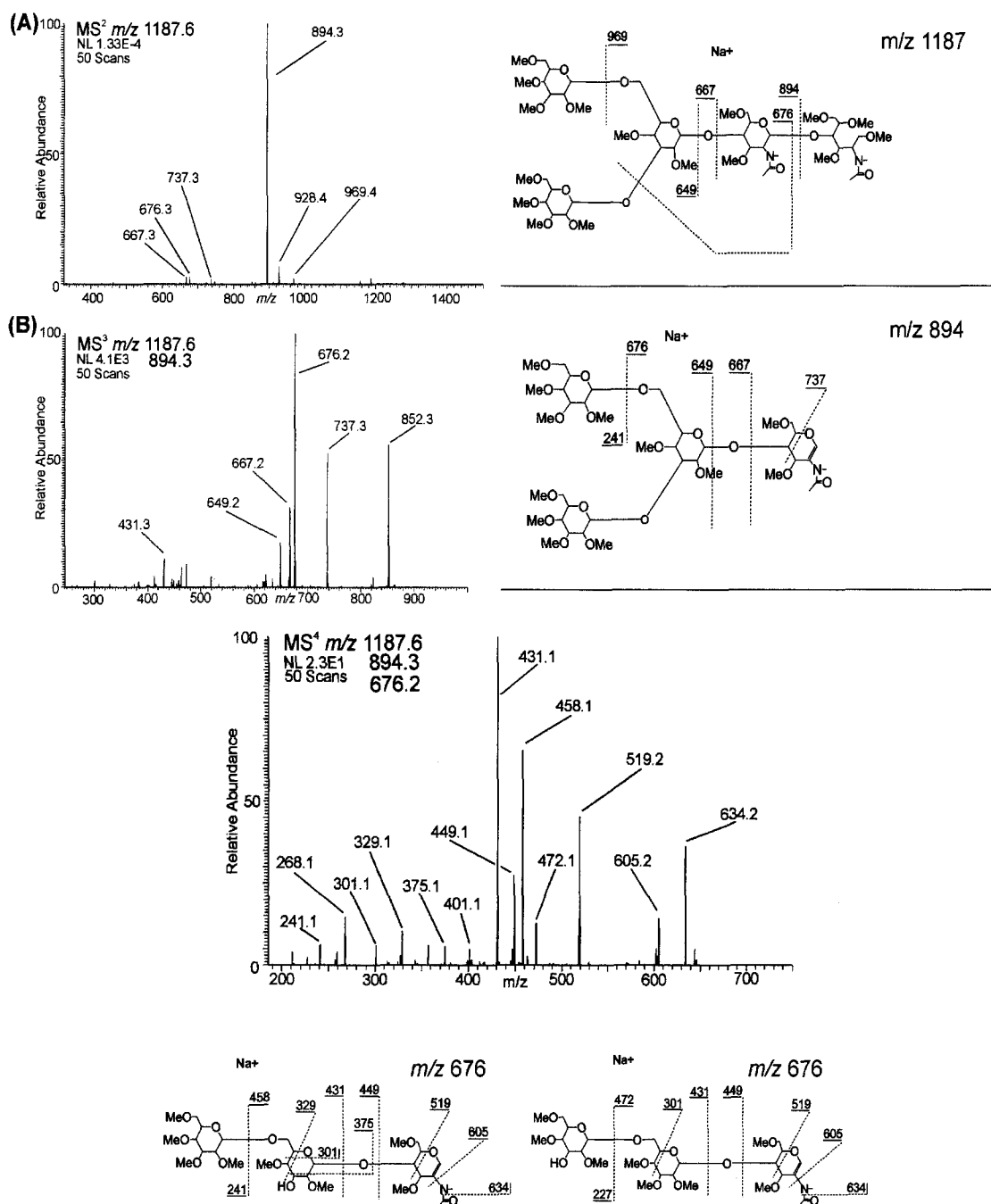


Figure 19. MS⁴ spectra of m/z 1187.6, Man₃GlcNAc₂ LLO from *C. elegans* and ion fragmentation assignment of the m/z 676 Y-type ion. The m/z 458 and m/z 472 indicate a mixture of linear and branching core structures.

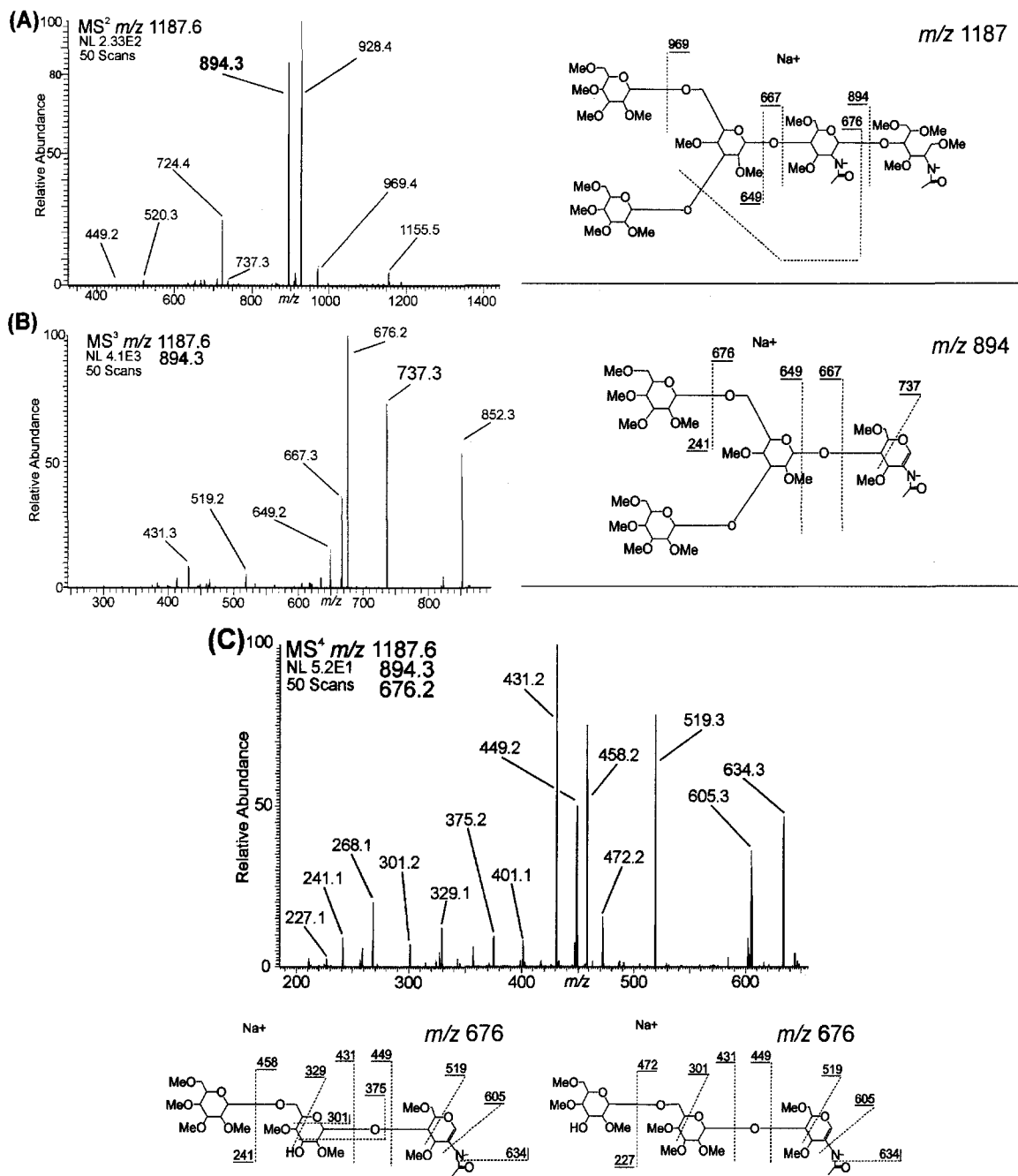


Figure 20. MS⁴ spectra of m/z 1187.6, Man₃GlcNAc₂ LLO from mouse macrophage cells and ion fragmentation assignments of the m/z 676 Y-type ion.

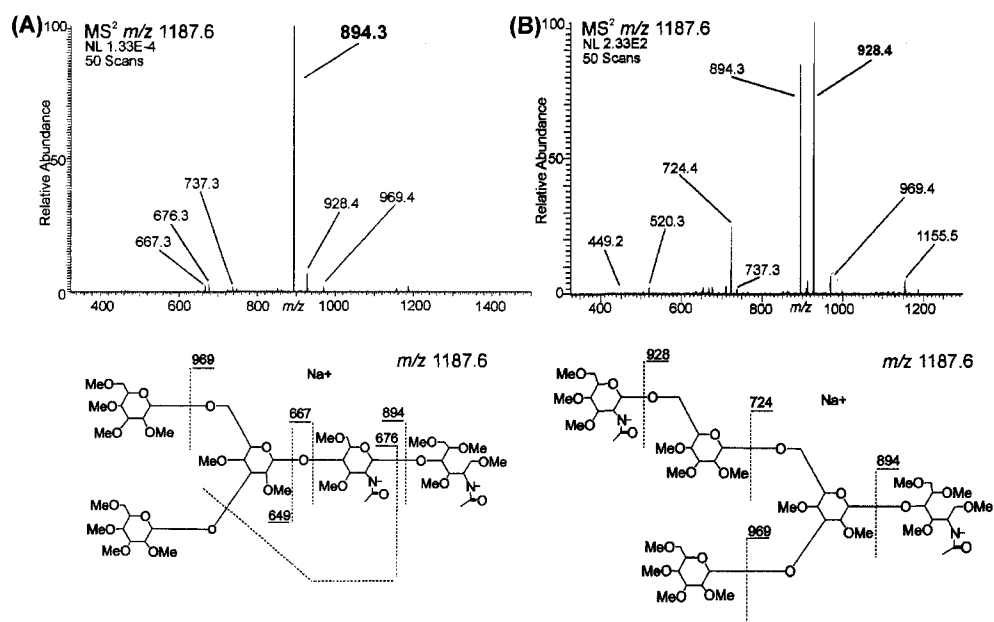


Figure 21. Comparison of the MS² spectra of the *m/z* 1187.6. In the *C. elegans* sample (panel A) *m/z* 894.3 is an expected peak representing the loss of a reducing end HexNAc. In the mouse macrophage sample (panel B), the major peak is *m/z* 928.4, only explainable by the loss of a terminal HexNAc.

Further investigation of the terminal HexNAc found in mouse macrophage suggests a core branching structure with the terminal HexNAc on the α 1,6 arm. This was identified by the MSⁿ pathway *m/z* 1187.6 \rightarrow *m/z* 928.4 \rightarrow *m/z* 724.5. At the MS⁴ level, the *m/z* 325 and *m/z* 375 suggest the α 1,6 linkage. The *m/z* 520 found in the MS³ spectra also reveals a linear structure. However, this was not confirmed at the MS⁴ level as the *m/z* 520 was not present.

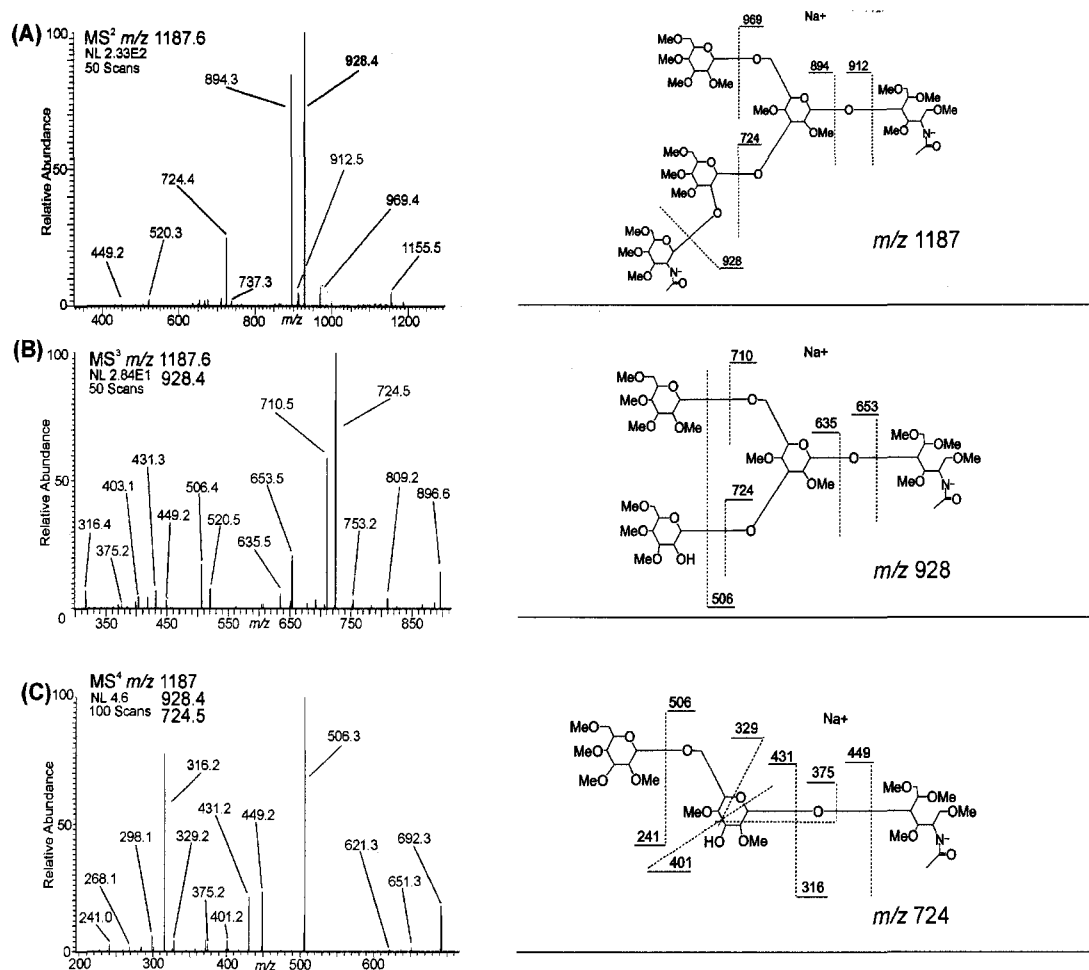


Figure 22. MS⁴ pathway of the m/z 1187 isolating the terminal HexNAc structure from mouse macrophage cells.

In summation, Man₃GlcNAc₂ LLO in the *C. elegans* and mouse macrophage is composed of 3 glycan structural isomers; the expected core branching structure, a linear core structure, and an unexpected terminal HexNAc structure.

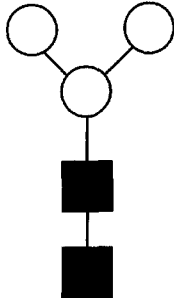
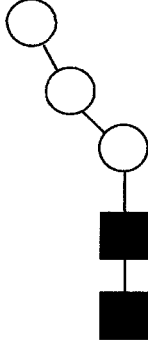
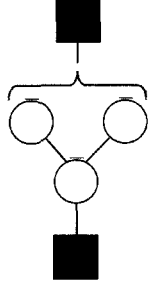
MS ⁿ Pathways- Man ₃ GlcNAc ₂ LLO		Consistent Topologies			
1187.6 → 969.5 (loss of ○-) → 676.3 (loss of ■) → 458.1		1			
1187.6 → 894.4 (loss of ■) → 676.3 (loss of ○-) → 458.1 (loss of ○-)		1			
1187.6 → 894.4 (loss of ■) → 737.3 → 519.2 (loss of ○-)		1			
1187.6 → 894.4 (loss of ■) → 667.2 → 563.2		2			
1187.6 → 894.4 (loss of ■) → 667.2 → 472.2		2			
1187.6 → 928.4 (loss of ■-)		3			
1		2		3	

Table 6. Table of the MSⁿ pathways analyzed and the corresponding topologies for *m/z* 1187.6, Man₃GlcNAc₂.

5.3.3 Comparative Structural Analysis Man₄GlcNAc₂ LLO

MSⁿ disassembly of the *m/z* 1391.6 ion in *C. elegans* revealed an unexpected tri-branching core isomer which was not seen in mouse macrophage cells. Both samples contained the typical core branching structure and the linear core structure uncovered in the Man₃GlcNAc₂ composition. The tri-branching structure was ascertained by the following MSⁿ pathway: *m/z* 1391.5 → *m/z* 1098.4 → *m/z* 880.3 → *m/z* 662.2.

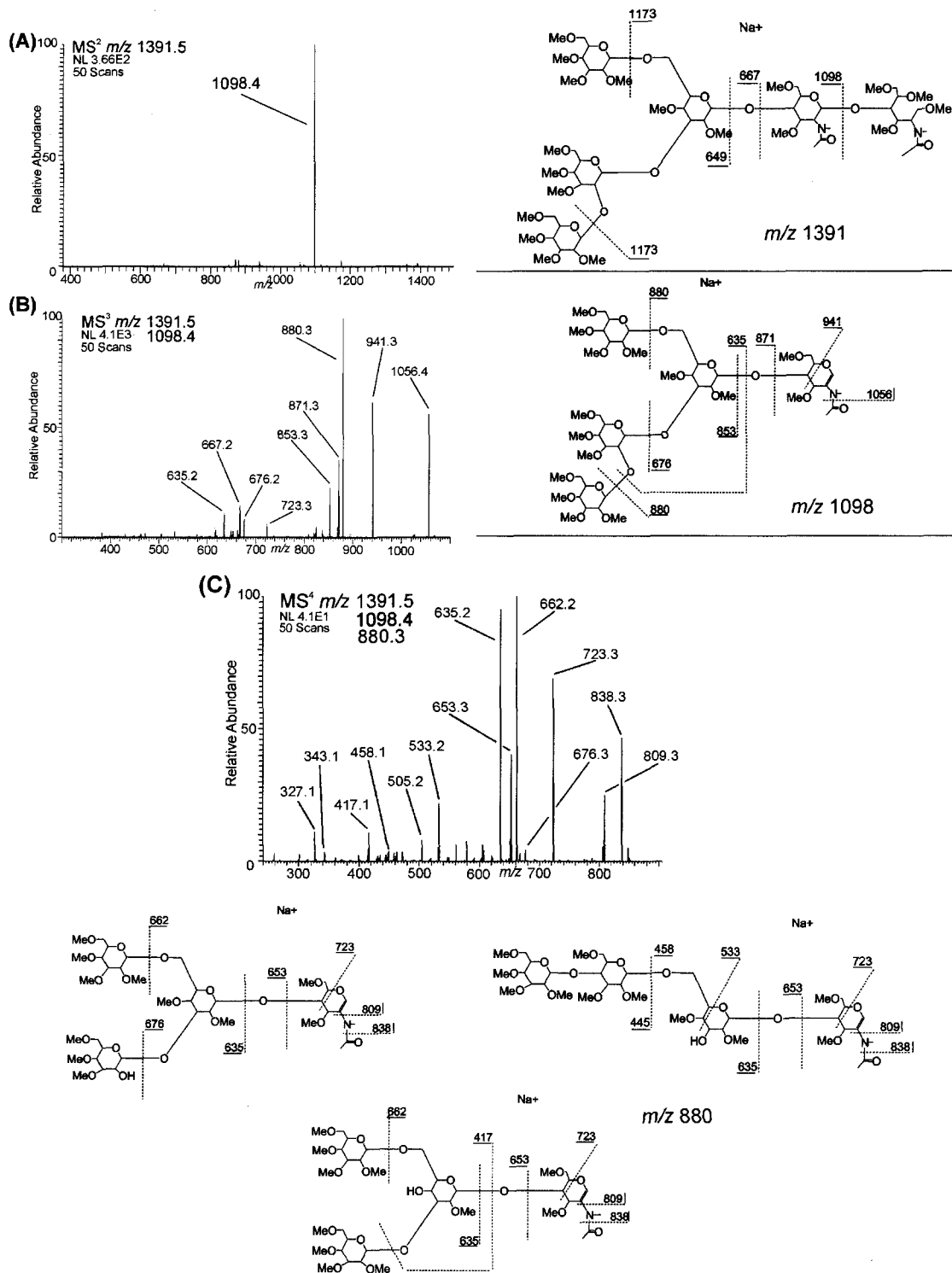


Figure 23. MS⁴ spectra of m/z 1391.5 Man₄GlcNAc₂ LLO from *C. elegans* and ion fragmentation of the m/z 880 Y-type ion.

Fragmentation of the m/z 880 (Y-type ion) indicated 3 possible structures. The m/z 676 originates from the loss of an internal hexose, while the m/z 662 represents the loss of a terminal hexose. The m/z 458 and m/z 472 were difficult to distinguish due to several peaks in that area of the spectra. Subsequent fragmentation of the m/z 662 (next figure) resolved this issue and aided in structural determination.

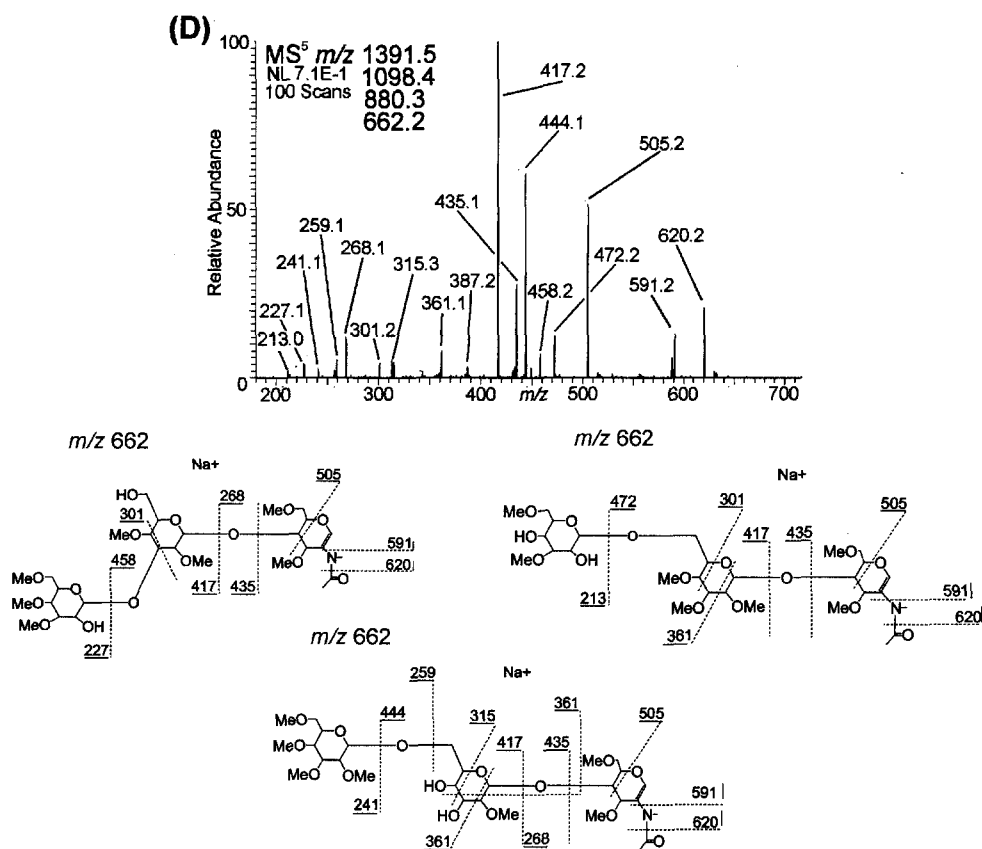


Figure 24. MS⁵ of m/z 1391.5, Man₄GlcNAc₂ LLO from *C. elegans*. Fragmentation of the m/z 662 revealed several unexpected ions.

Fragmentation of the m/z 662.2 (Y-type ion) produced an m/z 444 fragment only explainable by a tri-branching core. The m/z 472 peak is also

present suggesting a mixture of linear and tri-branched core structures. Since fragmentation of the m/z 662 was preceded by the loss of two terminal hexoses, the branching point must be present on the second mannose of either the α 1,6 or α 1,3 arm. This was supported by the m/z 213 peak, a hexose with 2 hydroxyls. In addition the m/z 667 peak at the MS³ level also points to a non-core branching structure. Finally the m/z 458 peak indicates the presence of the standard core branching isomer.

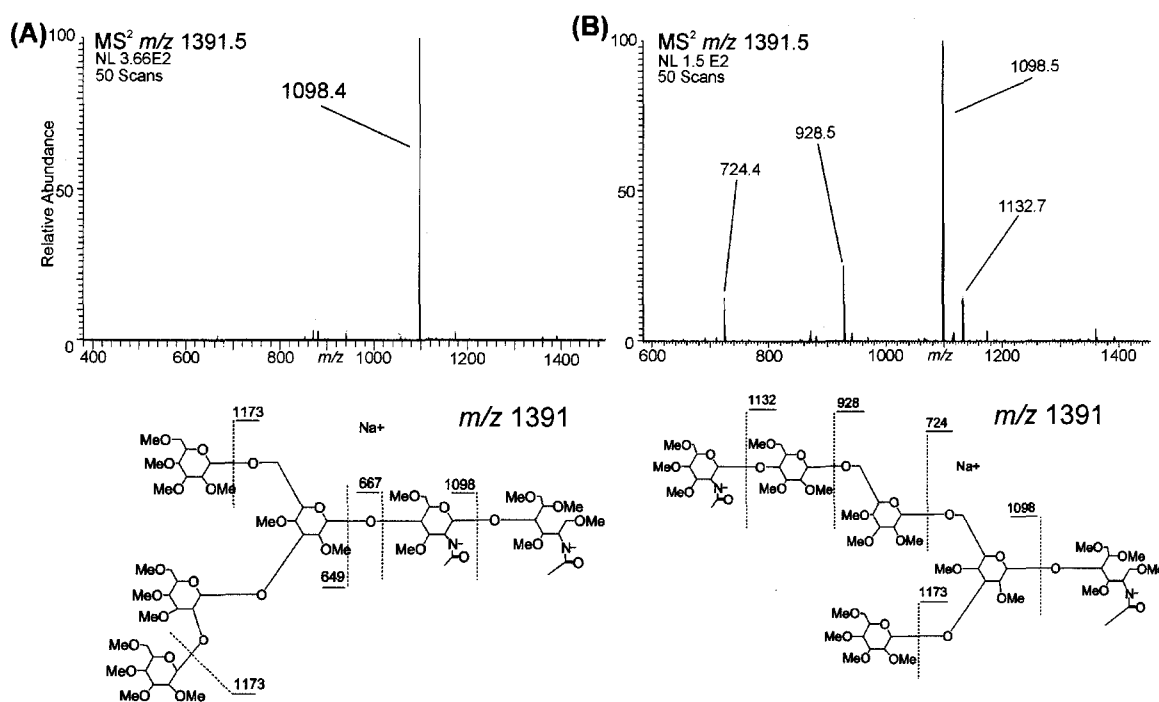


Figure 25. Comparison of the MS² spectra of m/z 1391.5, Man₄GlcNAc₂ LLO from *C. elegans* (panel A) and mouse macrophage(panel B).

The tri-branching core structure has been found on proteins in *C. elegans*, but unexpected in the LLO pathway. There was no evidence of this isomer in the mouse macrophage cells and only the core branching structure was

identified. However, MS² analysis again indicated the presence of a terminal HexNAc in the mouse macrophage cells.

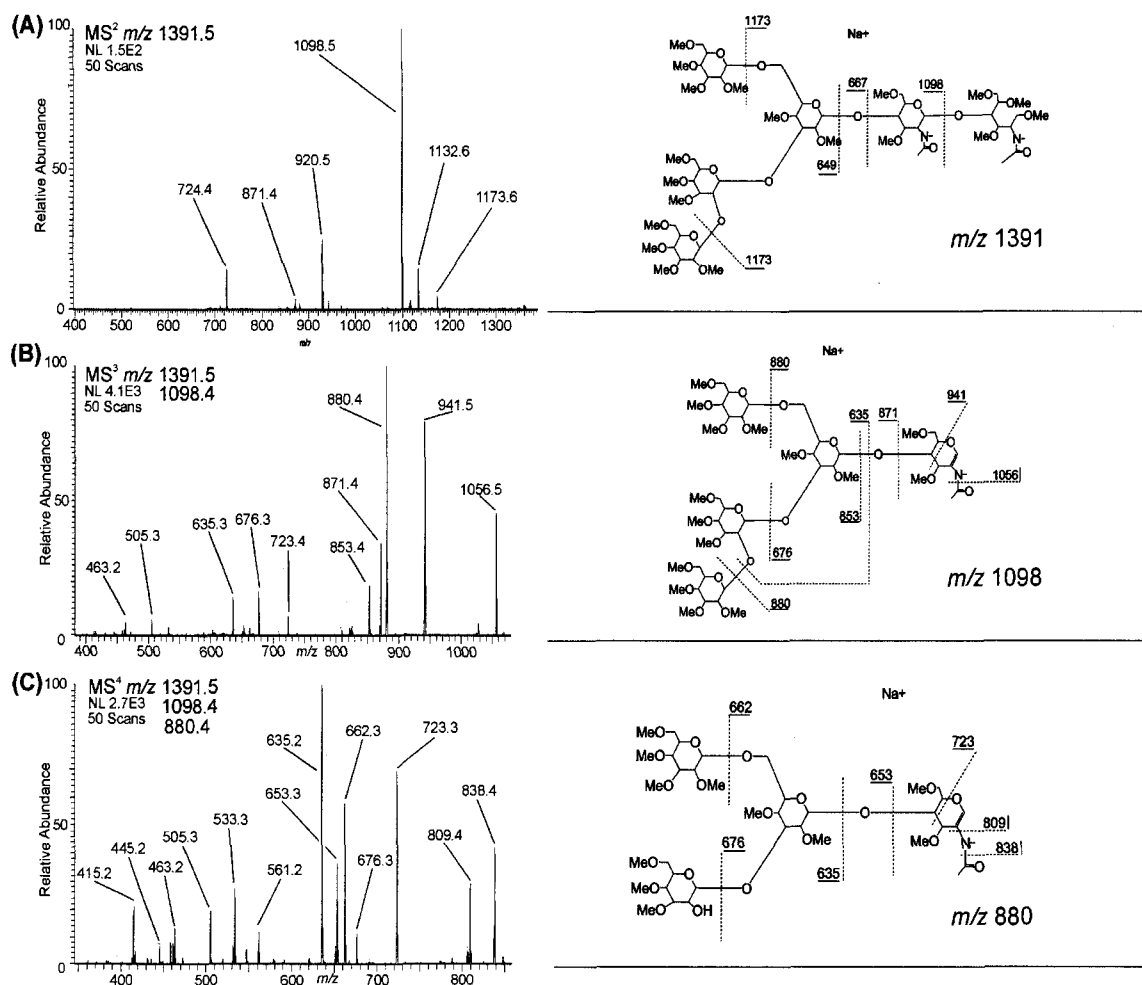


Figure 26. MS⁴ of the m/z 1391.5, Man₃GlcNAc₂ LLO from mouse macrophage cells.

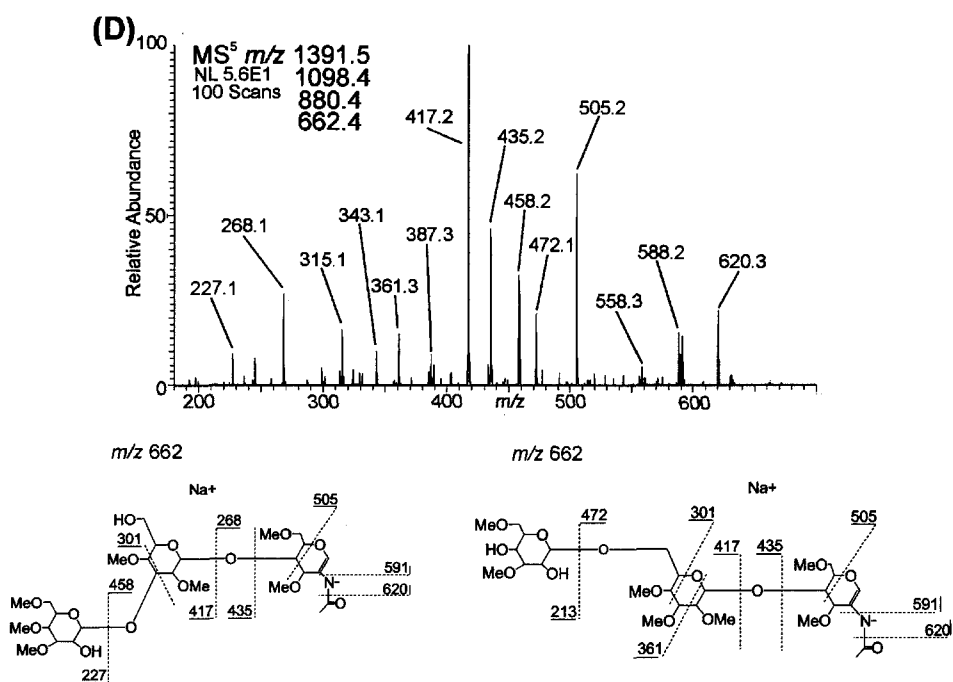


Figure 27. MS⁵ of the m/z 1391.5, Man₄GlcNAc₂ LLO from mouse macrophage cell and ion fragmentation assignment of the m/z 662 Y-type ion.

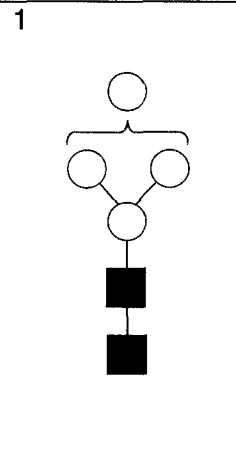
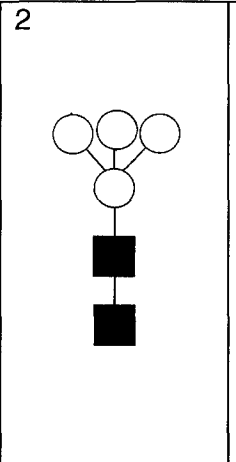
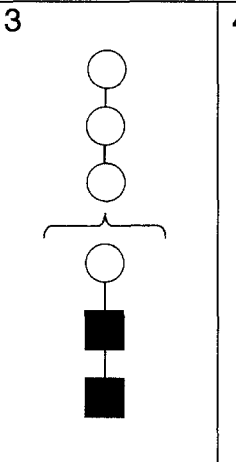
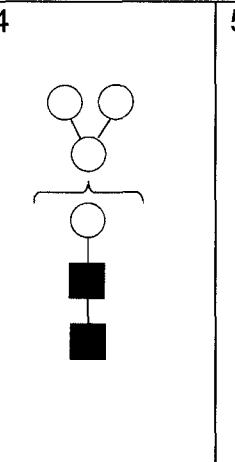
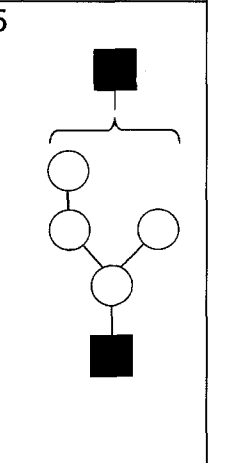
MS ⁿ Pathways- Man ₄ GlcNAc ₂ LLO					Consistent Topologies
1391.5 → 1098.4 (loss of ■) → 880.3 (loss of ○) → 662.2 (loss of ○)					1,2
1391.5 → 1098.4 (loss of ■) → 880.3 (loss of ○) → 662.2 (loss of ○) → 458.1 (loss of ○)					1
1391.5 → 1098.4 (loss of ■) → 880.3 (loss of ○) → 662.2 (loss of ○) → 444.1 (loss of ○)					2
1187.6 → 894.4 (loss of ■) → 667.2 → 563.2					2
1187.6 → 894.4 (loss of ■) → 676.2 → 472.2					3
1391.5 → 1098.4 (loss of ■) → 880.3 (loss of ○) → 662.2 (loss of ○) → 213.0					4
1187.6 → 928.4 (loss of ■)					5
1	2	3	4	5	
					

Table 7. Table of the MSⁿ pathways analyzed for Man₄GlcNAc₂ and the corresponding topologies. Structure 2 is unique to *C. elegans*.

5.3.4 Comparative Structural Analysis Man₅GlcNAc₂ LLO

The fragmentation pathway m/z 1595.8 → m/z 1302.6 → m/z 1084.4 → m/z 866.4 revealed the loss of two terminal hexoses and suggested a branching structure in the *C. elegans* sample. The loss of a third terminal hexose was observed at the MS⁵ level by the fragmentation of the m/z 866 → m/z 662. This indicated the presence of a branching structure similar to the standard Man₅GlcNAc₂ glycan found on proteins.

The expected LLO structure contains only one branching point at the first mannose and should only allow for the loss of two terminal hexoses. The α 1,6 branch should not be completed until $\text{Man}_7\text{GlcNAc}_2$ in LLO samples. The fragmentation pathway m/z 1595.8 \rightarrow m/z 1302.6 \rightarrow m/z 1084.4 \rightarrow m/z 880 suggested the presence of the expected $\text{Man}_5\text{GlcNAc}_2$ structure. However, the ion products m/z 505, m/z 519 and m/z 533 from the fragmentation of the m/z 880 suggest an extension on the α 1,6 arm.

Careful review of the data suggested several additional unexpected structures. The m/z 472 peak was observed at the MS^6 level by the fragmentation pathway m/z 1595.8 \rightarrow m/z 1302.6 \rightarrow m/z 1084.4 \rightarrow m/z 866 \rightarrow m/z 648. The production of both the m/z 472 and m/z 458 ions proposes a mixture of branched and linear cores, a reiterated pattern seen in *C. elegans* LLO. However, a completely linear structure was unable to fully explain several fragmentation pathways since the m/z 880 and m/z 866.4 fragments suggest a branching structure. In addition, it was possible for the m/z 1302.6 to lose 3 terminal hexoses. Therefore, a tri-branching type structure was also proposed and is supported by several fragmentation pathways. If the tri-branch occurs at the second hexose, the m/z 472 can still be produced from the fragmentation of the m/z 648. Furthermore, this structure is supported by the m/z 871 ion produced from the fragmentation of the m/z 1302 peak at the MS^2 level. Unfortunately, this structure was not completely confirmed through analysis of the m/z 871 due to limited sample amount. Interestingly, the m/z 444 ion is

again present at MS⁶ of the *m/z* 648 which suggested the possibility of the tri-branching core previously identified in the Man₄GlcNAc₂ composition.

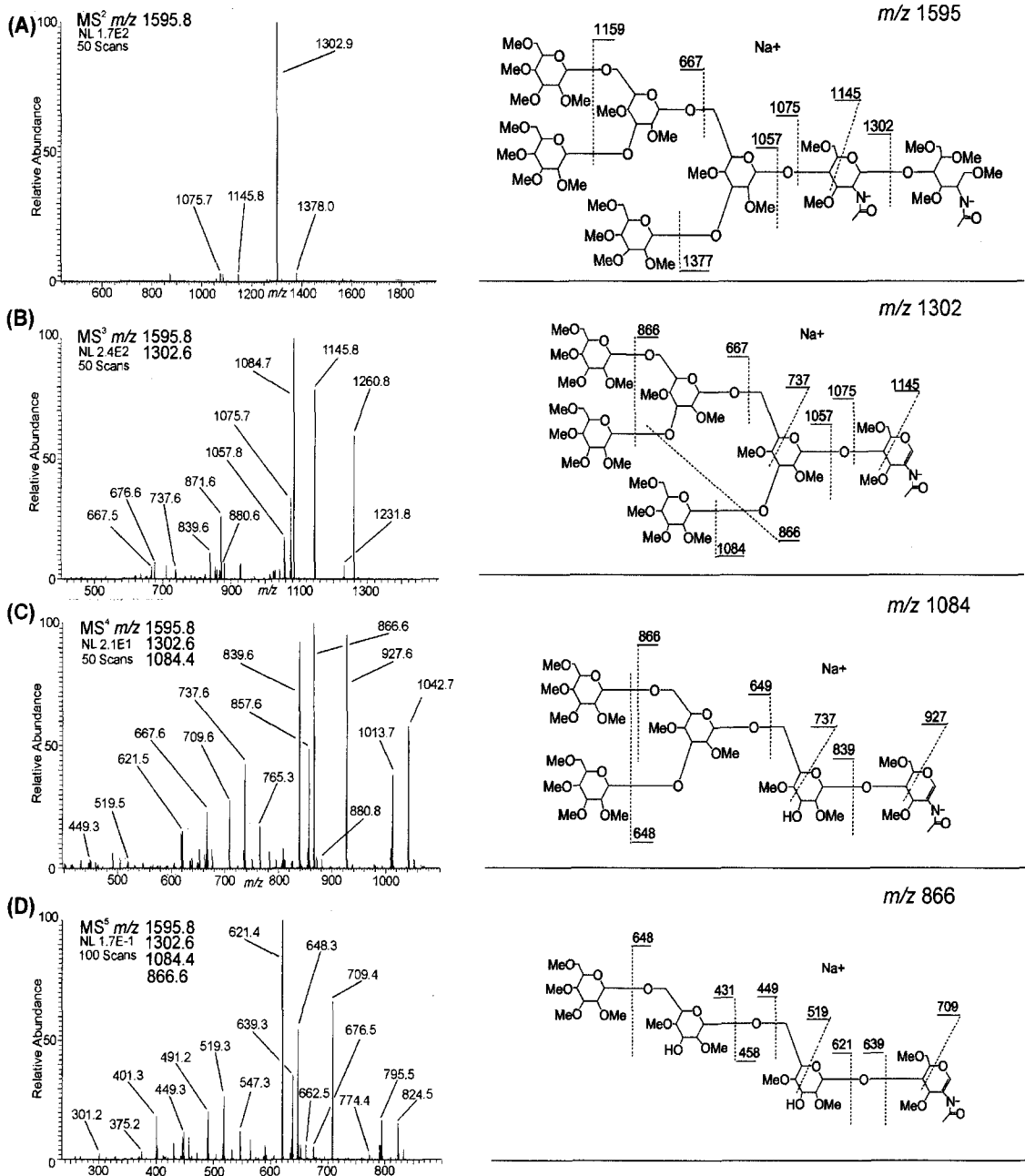


Figure 28. MS⁵ of the *m/z* 1595.8, Man₅GlcNAc₂ LLO from *C. elegans* and ion fragmentation assignment of the *m/z* 866 Y-type ion. This fragmentation pathway suggests a structure similar to the Man₅GlcNAc₂ commonly found on proteins.

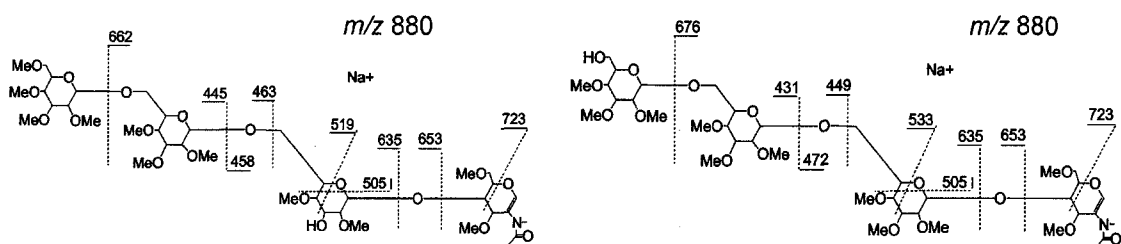
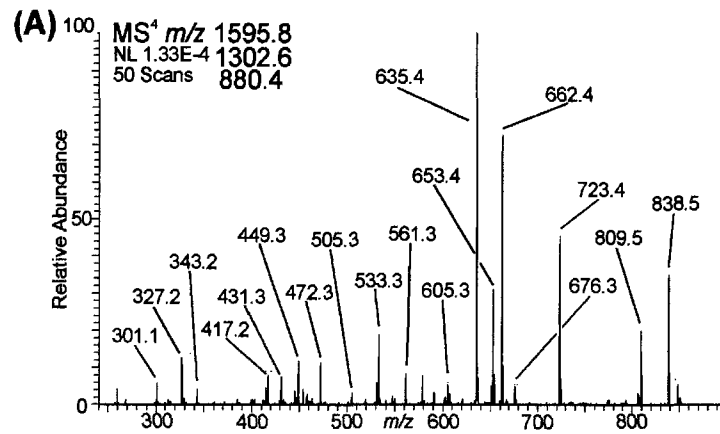


Figure 29. MS⁴ of the m/z 1595.8, Man₅GlcNAc₂ LLO from *C. elegans* and ion fragmentation assignment of the m/z 880Y-type ion. Fragmentation of the m/z 880 ion suggests the presence of two core isomers. The m/z 676, m/z 505 and m/z 472 are indicative of a linear structure. The m/z 505, m/z 519 and, m/z 533 suggest this extension is attached to the α 1,6 arm.

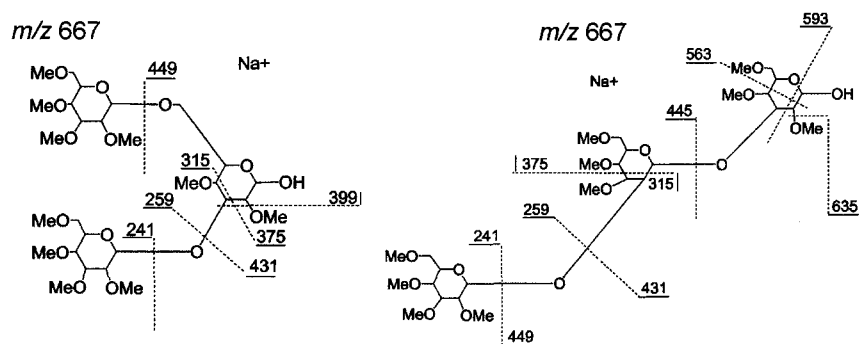
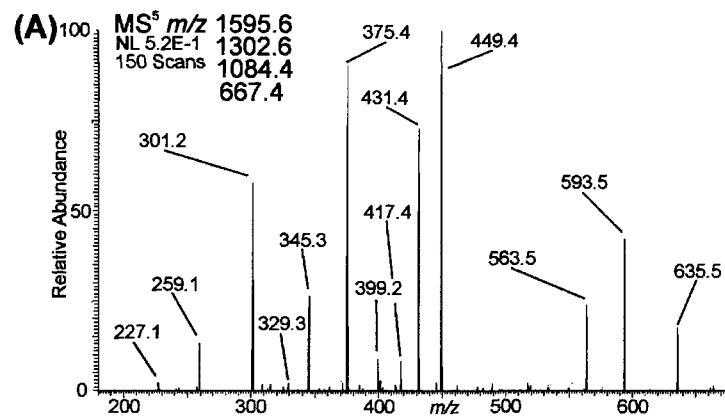


Figure 30. MS⁵ of the m/z 1595.8, Man₃GlcNAc₂ LLO from *C. elegans* and ion fragmentation assignment of the m/z 667.

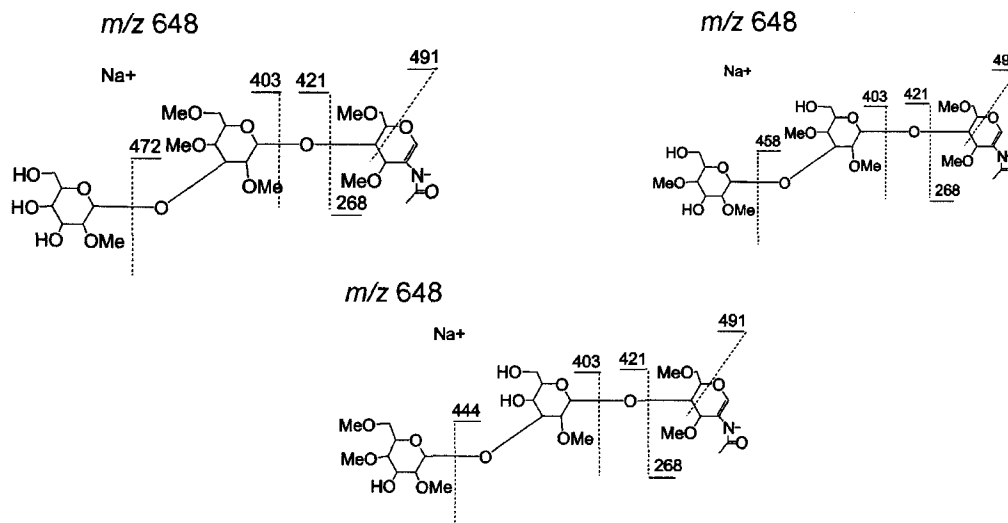
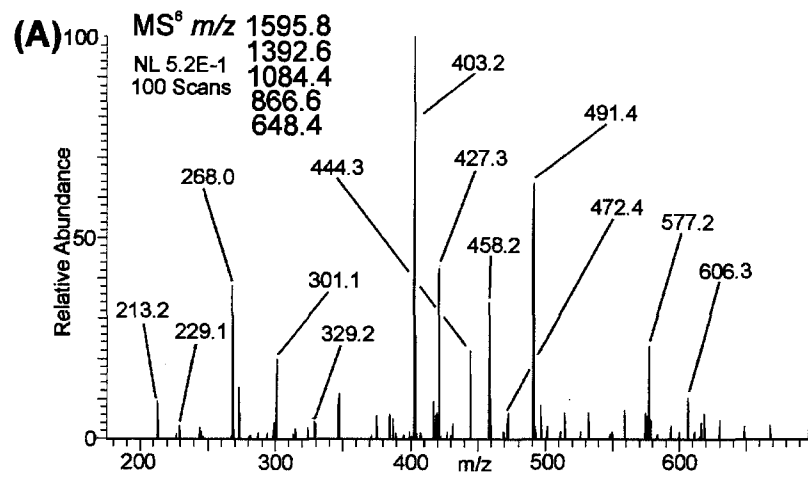


Figure 31. MS⁶ of the m/z 1595.8, Man₃GlcNAc₂ LLO from *C. elegans* and ion fragmentation assignment of the m/z 648 Y-ion.

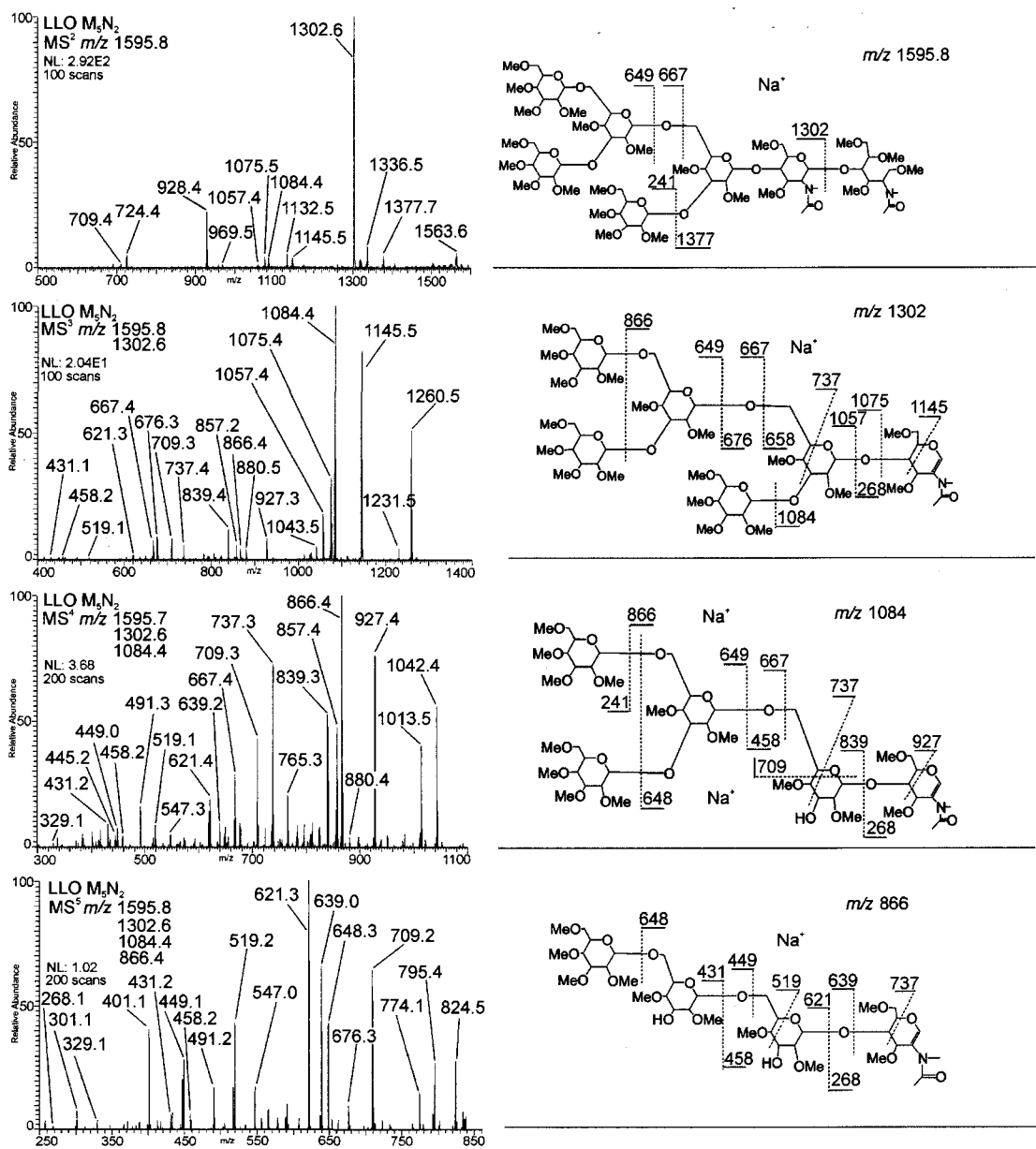


Figure 32. MS⁵ of *m/z* 1595.8, *Man*₅*GlcNAc*₂ LLO from mouse macrophage cells.

MSⁿ disassembly of *m/z* 1595.8, *Man*₅*GlcNAc*₂, isolated from the mouse macrophage cell line indicates 3 structures are present. The fragmentation pathway, *m/z* 1595.8 → *m/z* 1302.6 → *m/z* 1084.4 → *m/z* → *m/z* 866.4 is consistent with the branching structure found in *C. elegans*. Again, this structure

is normally found on proteins after Golgi processing. The fragmentation of the m/z 667 supports this branching structure. The fragmentation pathway m/z 1595.8 \rightarrow m/z 1302.6 \rightarrow m/z 1084.4 \rightarrow m/z 880 indicates core branching pattern found in the expected LLO structures. The linear and tri-branching core was not observed in the mouse macrophage sample in the $\text{Man}_5\text{GlcNAc}_2$ composition. However, the loss of the terminal HexNAc was observed at the MS^2 level.

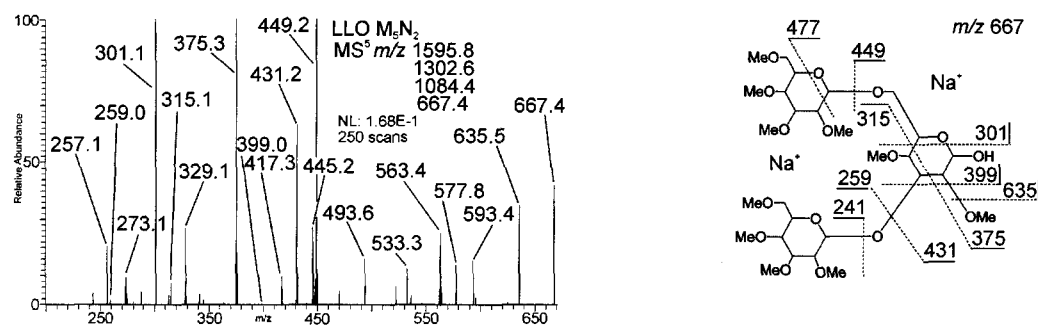


Figure 33. MS^5 of m/z 1595.8, $\text{Man}_5\text{GlcNAc}_2$ from mouse macrophage cells and ion fragmentation of the m/z 667 C-type ion.

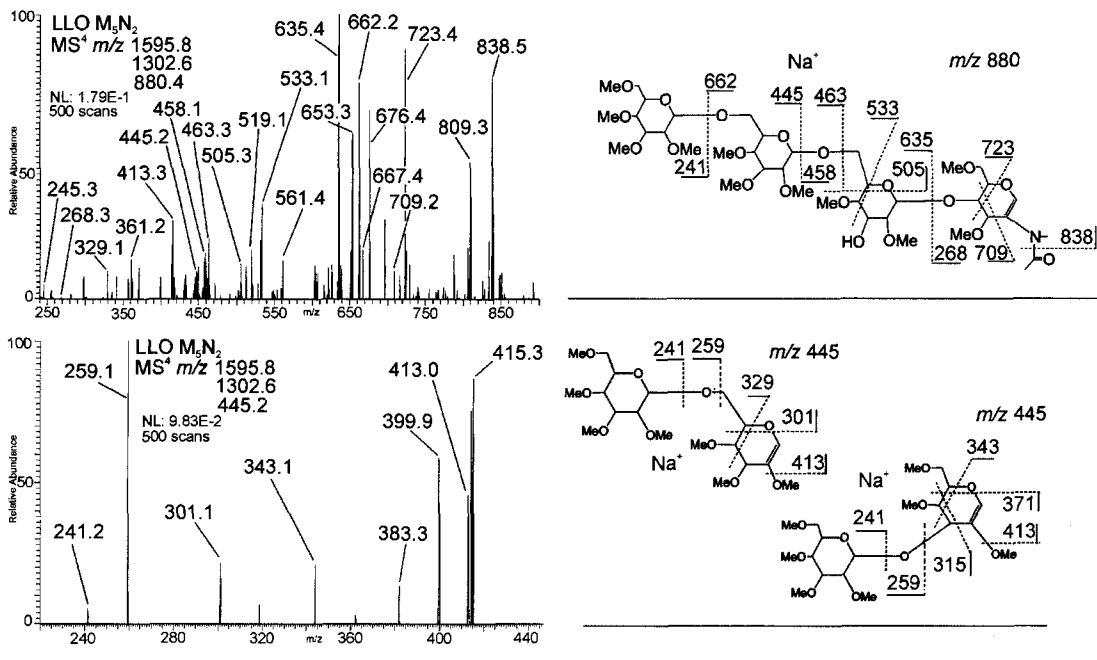


Figure 34. MS⁵ of m/z 1595.8, Man₅GlcNAc₂ from mouse macrophage cells and ion fragmentation of the m/z 880 Y-type ion and m/z 445 B-type ion.

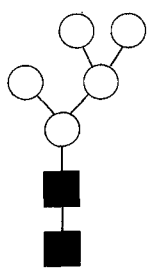
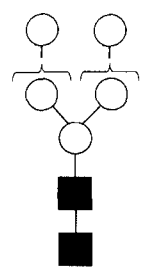
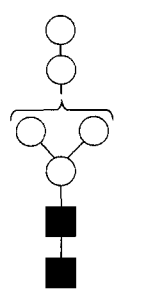
MS ⁿ Pathways Man ₅ GlcNAc ₂ LLO		Consistent Topologies
1595.8 → 1377.7 (loss of ○-) → 1084.4 (loss of ■) → 866.4 (loss of ○-) → 648.2 (loss of ○-) → 458.1 (○-■)		1
1595.8 → 1377.7 (loss of ○-) → 1159.6 (loss of ○-) → 941.6 (loss of ○-) → 648.2 (loss of ■)		1
1595.8 → 1377.7 (loss of ○-) → 1084.4 (loss of ■) → 667.4 (○-○-○-, C ₃ -type ion) → 375.1		1
1595.8 → 1302.6 (loss of ■) → 1084.4 (loss of ○-) → 667.4 (○-○-○-, C ₃ -type ion) → 563.4		3
1595.8 → 1302.6 (loss of ■) → 1084.4 (loss of ○-) → 667.4 (○-○-○-, C ₃ -type ion) → 227 (-○-)		3
1595.8 → 1377.7 (loss of ○-) → 1084.4 (loss of ■) → 866.4 (loss of ○-) → 662.1 (loss of -○-)		3
1595.8 → 1377.7 (loss of ○-) → 1084.4 (loss of ■) → 866.4 (loss of ○-) → 621.3 (loss of ■) → 417.0		3
1595.8 → 1377.7 (loss of ○-) → 1084.4 (loss of ■) → 866.4 (loss of ○-) → 621.3 (loss of ■) → 227.0 (-○-)		3
1595.8 → 880.4 → 667.4 (○-○-○-)		3
1595.8 → 445.3 (○-○-, B ₂ -type ion) → 301		2,3
1595.8 → 445.3 (○-○-, B ₂ -type ion) → 343.1		2,3
1595.8 → 1302.6 (loss of ■) → 1084.4 (loss of ○-) → 880.4 (loss of -○-)		2,3
1595.8 → 1302.6 (loss of ■) → 1084.4 (loss of ○-) → 880.4 (loss of -○-) → 635.3 (loss of ■) → 533.1		2
1595.8 → 1302.6 (loss of ■) → 1084.4 (loss of ○-) → 880.4 (loss of -○-) → 635.3 (loss of ■) → 547.3		2
1595.8 → 1302.6 (loss of ■) → 1084.4 (loss of ○-) → 880.4 (loss of -○-) → 662.4 (loss of ○-)		2
1595.8 → 547.3 (^{3,5} A ₂ ion) → 241.0 (○-)		2,3
1595.8 → 547.3 (^{3,5} A ₂ ion) → 329.1 (loss of ○-)		2,3
1	2	3
		

Table 8. Table of the MSⁿ pathways analyzed and the corresponding topologies

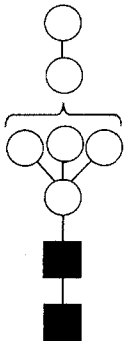
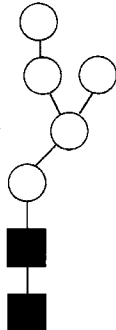
MS ⁿ Pathways Man ₅ GlcNAc ₂ LLO		Consistent Topologies
1595.8 → 1302.6 (loss of ■) → 1084.4 (loss of ○) → 866.4 (loss of ○) → 648.4 (loss of ○) → 444.3		5
1595.8 → 1302.6 (loss of ■) → 1084.4 (loss of ○) → 866.4 (loss of ○) → 648.4 (loss of ○) → 472.3		6
1595.8 → 1302.6 (loss of ■) → 871.6(○○○○)		5,6
	6 	

Table 9. Table of the MSⁿ pathways analyzed and the corresponding topologies

5.4 Future Directions

The next direction of this project would be to continue with LLO comparative structural analysis targeting specific molecular compositions with biological significance in mind. The most interesting target would be the mature precursor Glc₃Man₉GlcNAc₂. However, the lack of LLO material prevents extensive MSⁿ analysis required for such a large structure. Very large scale extractions would be required to properly isolate enough material to investigate the larger LLOs.

Isolation of dolichol linked glycans by liquid-liquid extractions is probably not exclusive to LLOs. Free glycans, glycosphingolipids and other lipid linked

glycan are most likely extracted as well. Dialysis of the extracts should remove any lower molecular weight molecules, eliminating the majority of free glycans normally found in the cytosol. However, MSⁿ analysis of the intact precursor would be the next suitable course of action to confirm results reported here. MS² of the entire LLO precursor has been completed by other laboratories. Larger molecular weights and various dolichol repeating units confound the identification through MS. Dol(19)-pp- GlcNAc₂Man₉Glc₃ has been identified as the major constituent (Garrett, Guan et al. 2007). Intact LLO MSⁿ analysis was attempted without any success.

Another issue to address would be the relationship between the LLOs and glycans found on glycoproteins. As stated earlier, the exoglycosidases of the ER and Golgi are capable of extensively trimming down the transferred glycan precursor and this is believed to always occur with the exception of non secreted ER resident glycoproteins. Therefore, there are two experiments to address this issue. Exoglycosidase inhibitors such as castanospermine could be used to prevent trimming of transferred glycans *in vivo*. Following a certain incubation time with these inhibitors the N-glycans could be released from the glycoproteins protein and analyzed via MSⁿ. This should be able to identify the primary isomers that are at least transferred to the glycoprotein. Secondly, ER resident proteins containing high mannose type glycans could also be targeted for study. This would have to involve a targeting and purification of specific glycoproteins most likely with the use of affinity chromatography prior to MSⁿ analysis.

Once the isomers of the LLO pathway are extensively catalogued comparisons could be made to diseased states. For example, wild type mouse macrophage cells could be compared to cancerous cells. As many of the glycosylation pathways appeared altered in cancerous states it is likely the LLO pathway is aberrant under changes in cellular metabolism.

5.5 Conclusions

Identifying structural isomers in the LLO pathway highlights the unknown degree of variability associated with *N*-glycosylation. Although, this data cannot directly prove any biological significance, it questions decade old theory believed to be factual. LLO structural isomers may not have a large impact on the overall biology of the cell, especially if they are simply discarded.

This project identified several structural isomers in the series $\text{Man}_3\text{GlcNAc}_2$ through $\text{Man}_5\text{GlcNAc}_2$. The overall pattern in *C. elegans* suggests increasing structural diversity with an increase in carbohydrate residues. This also applies to mouse macrophage cell albeit to a lesser extent. The unique tri-branching structure identified in *C. elegans* could not be found in the mouse macrophage cells. However, mouse macrophage cells contain an unexpected terminal HexNAc structure. Interestingly, the linear glycan appears in both *C. elegans* and mouse macrophage samples. However, in the mouse macrophage, the linear core structure was only identified in the $\text{Man}_3\text{GlcNAc}_2$ composition.

LLO structural isomers isolated from *C. elegans*

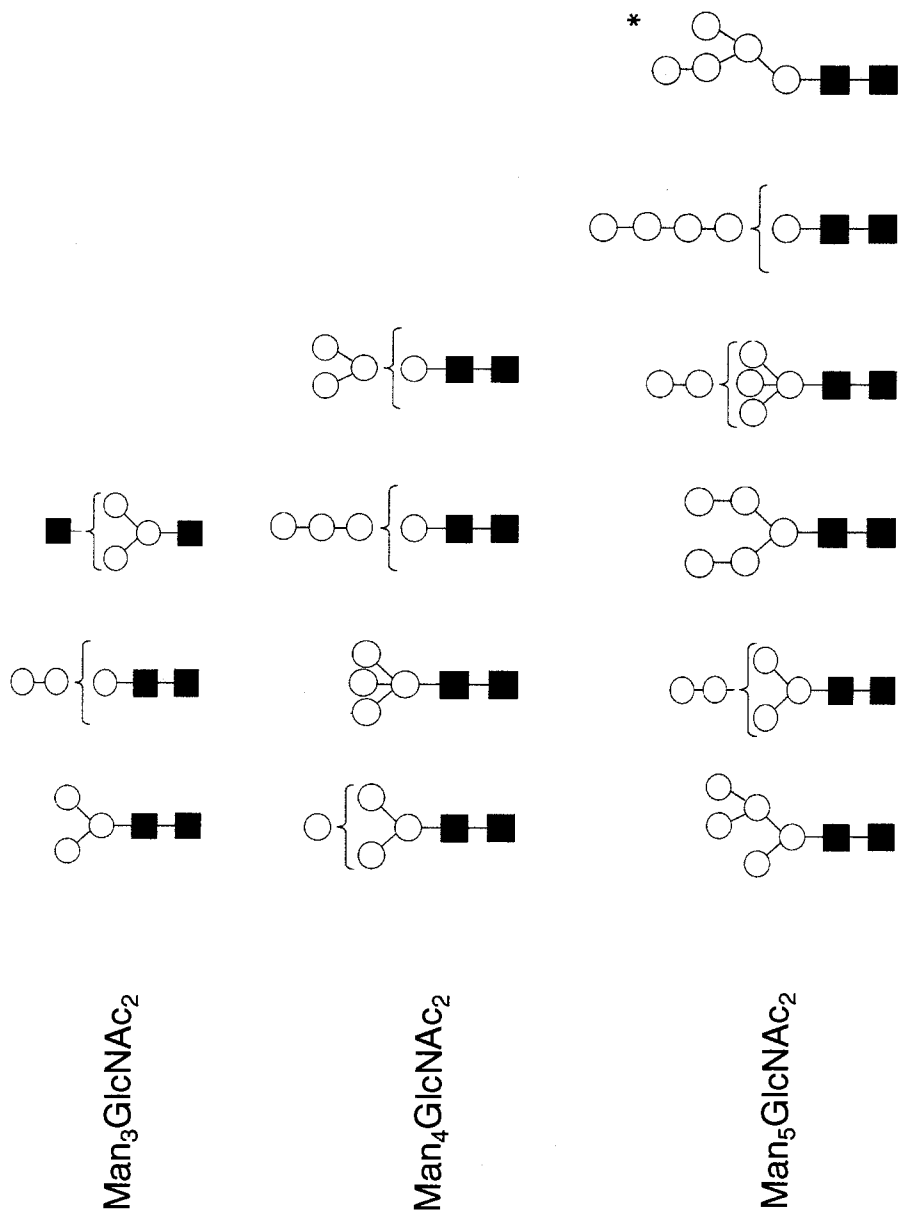


Figure 35. LLO structural isomers isolated for each molecular composition from *C. elegans*.

LLO structural isomers isolated from mouse macrophage cells

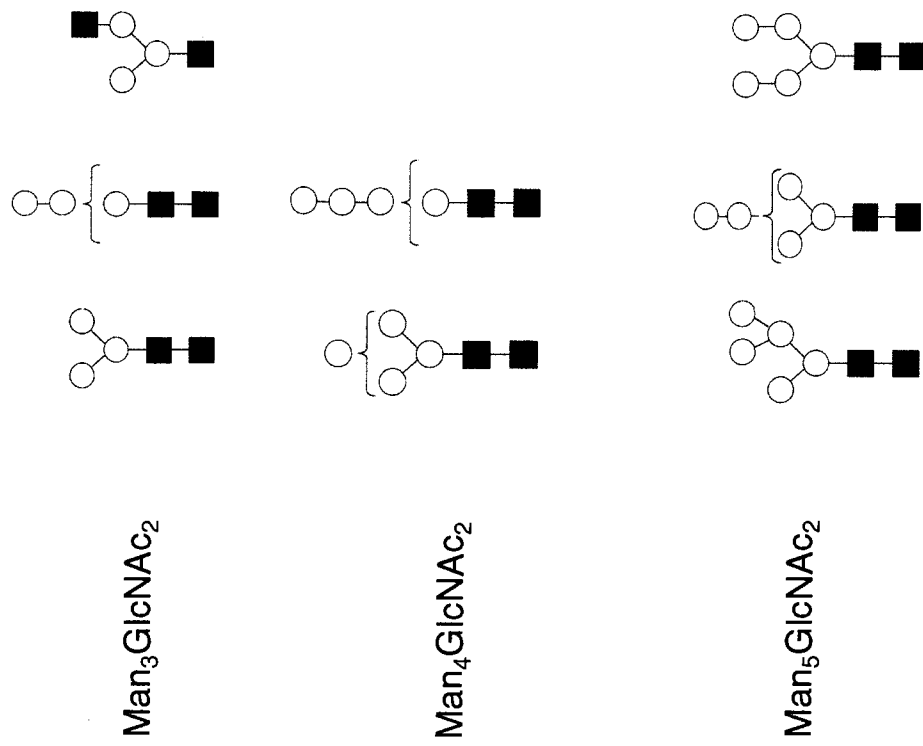


Figure 36. LLO structural isomers isolated for each molecular composition from mouse macrophage cells.

The widely accepted LLO standard tri-mannosyl core was identified in both samples. This could be the primary structure that is synthesized by the LLO pathway. However, the number of other isomers identified questions the overall specificity of the enzymes of this pathway. In addition, these isomers would not be detected by HPLC or other glycoanalytic techniques that do not employ MSⁿ. Therefore, they must be considered when interpreting data from these methods. Even if they are identified as free glycans or products of degradation they will contribute to results obtained by non MSⁿ methods since the extraction protocol followed here was adapted from other methods.

In summary the MSⁿ techniques employed here provided a detailed structural analysis of the isolated carbohydrates. The results indicate a range of different structural isomers for each molecular composition. Although the source of these isomers is questionable, their presence is obvious. Hopefully continual investigation of the LLO pathway with techniques described here will aid in the elucidation and understanding of *N*-glycosylation.

REFERENCES

- (1998). "Genome sequence of the nematode *C. elegans*: a platform for investigating biology." Science **282**(5396): 2012-2018.
- Abeijon, C. and C. B. Hirschberg (1992). "Topography of glycosylation reactions in the endoplasmic reticulum." Trends Biochem Sci **17**(1): 32-36.
- Ashline, D., S. Singh, et al. (2005). "Congruent Strategies for Carbohydrate Sequencing. 1. Mining Structural Details by MSn." Analytical Chemistry **77**(17): 6250-6262.
- Ashline, D. J., A. J. Lapadula, et al. (2007). "Carbohydrate structural isomers analyzed by sequential mass spectrometry." Anal Chem **79**(10): 3830-3842.
- Barone, R., L. Sturiale, et al. (2009). "Mass spectrometry in the characterization of human genetic N-glycosylation defects." Mass Spectrom Rev **28**(3): 517-542.
- Brenner, S. (1974). "The genetics of *Caenorhabditis elegans*." Genetics **77**(1): 71-94.
- Burda, P. and M. Aebi (1998). "The ALG10 locus of *Saccharomyces cerevisiae* encodes the alpha-1,2 glucosyltransferase of the endoplasmic reticulum: the terminal glucose of the lipid-linked oligosaccharide is required for efficient N-linked glycosylation." Glycobiology **8**(5): 455-462.
- Burda, P. and M. Aebi (1999). "The dolichol pathway of N-linked glycosylation." Biochim Biophys Acta **1426**(2): 239-257.
- Chalfie, M., H. R. Horvitz, et al. (1981). "Mutations that lead to reiterations in the cell lineages of *C. elegans*." Cell **24**(1): 59-69.
- Cho, J. H., K. M. Ko, et al. (2007). "Functional importance of polymerization and localization of calsequestrin in *C. elegans*." J Cell Sci **120**(Pt 9): 1551-1558.
- Cho, J. H., Y. S. Oh, et al. (2000). "Calsequestrin, a calcium sequestering protein localized at the sarcoplasmic reticulum, is not essential for body-wall muscle function in *Caenorhabditis elegans*." J Cell Sci **113** (Pt 22): 3947-3958.

- Cipollo, J. F. and R. B. Trimble (2002). "Hypoglycosylation in the alg12delta yeast mutant destabilizes protease A and causes proteolytic loss of external invertase." Glycobiology **12**(11): 30G-33G.
- Ciucanu, I. and F. Kerek (1984). "A simple and rapid method for the permethylation of carbohydrates." Carbohydrate Research **131**: 209-217.
- Frank, C. G. and M. Aebi (2005). "ALG9 mannosyltransferase is involved in two different steps of lipid-linked oligosaccharide biosynthesis." Glycobiology **15**(11): 1156-1163.
- Freeze, H. H. (2001). "Update and perspectives on congenital disorders of glycosylation." Glycobiology **11**(12): 129R-143R.
- Freeze, H. H. (2007). "Congenital Disorders of Glycosylation: CDG-I, CDG-II, and beyond." Curr Mol Med **7**(4): 389-396.
- Gao, N. and M. A. Lehrman (2002). "Analyses of dolichol pyrophosphate-linked oligosaccharides in cell cultures and tissues by fluorophore-assisted carbohydrate electrophoresis." Glycobiology **12**(5): 353-360.
- Garrett, T. A., Z. Guan, et al. (2007). "Analysis of ubiquinones, dolichols, and dolichol diphosphate-oligosaccharides by liquid chromatography-electrospray ionization-mass spectrometry." Methods Enzymol **432**: 117-143.
- Grubenmann, C. E., C. G. Frank, et al. (2004). "Deficiency of the first mannosylation step in the N-glycosylation pathway causes congenital disorder of glycosylation type I_k." Hum Mol Genet **13**(5): 535-542.
- Hanneman, A. J., J. C. Rosa, et al. (2006). "Isomer and glycomer complexities of core GlcNAcs in *Caenorhabditis elegans*." Glycobiology **16**(9): 874-890.
- Henry, H., F. Froehlich, et al. (1999). "Microheterogeneity of Serum Glycoproteins in Patients with Chronic Alcohol Abuse Compared with Carbohydrate-deficient Glycoprotein Syndrome Type I." Clinical Chemistry **45**(9): 1408-1413.
- Hirschberg, C. B. and M. D. Snider (1987). "Topography of glycosylation in the rough endoplasmic reticulum and Golgi apparatus." Annu Rev Biochem **56**: 63-87.

- Hubbard, S. C. and R. J. Ivatt (1981). "Synthesis and processing of asparagine-linked oligosaccharides." Annu Rev Biochem **50**: 555-583.
- Huffaker, T. C. and P. W. Robbins (1982). "Temperature-sensitive yeast mutants deficient in asparagine-linked glycosylation." J Biol Chem **257**(6): 3203-3210.
- Jaeken, J. and H. Carchon (2001). "Congenital disorders of glycosylation: the rapidly growing tip of the iceberg." Curr Opin Neurol **14**(6): 811-815.
- Jaeken, J. and G. Matthijs (2001). "Congenital disorders of glycosylation." Annu Rev Genomics Hum Genet **2**: 129-151.
- Kelleher, D. J. and R. Gilmore (2006). "An evolving view of the eukaryotic oligosaccharyltransferase." Glycobiology **16**(4): 47R-62R.
- Kelleher, D. J., D. Karaoglu, et al. (2001). "Large-scale isolation of dolichol-linked oligosaccharides with homogeneous oligosaccharide structures: determination of steady-state dolichol-linked oligosaccharide compositions." Glycobiology **11**(4): 321-333.
- Knauer, R. and L. Lehle (1999). "The oligosaccharyltransferase complex from yeast." Biochim Biophys Acta **1426**(2): 259-273.
- Kornfeld, R. and S. Kornfeld (1985). "Assembly of asparagine-linked oligosaccharides." Annu Rev Biochem **54**: 631-664.
- Lehle, L., S. Strahl, et al. (2006). "Protein glycosylation, conserved from yeast to man: a model organism helps elucidate congenital human diseases." Angew Chem Int Ed Engl **45**(41): 6802-6818.
- Lehrman, M. A. and N. Gao (2003). "Alternative and sources of reagents and supplies of fluorophore-assisted carbohydrate electrophoresis(FACE)." Glycobiology **13**(1): 1G-3G.
- Marquardt, T. and H. Freeze (2001). "Congenital disorders of glycosylation: glycosylation defects in man and biological models for their study." Biol Chem **382**(2): 161-177.
- Matthijs, G., E. Schollen, et al. (2000). "Mutations in PMM2 that cause congenital disorders of glycosylation, type Ia (CDG-Ia)." Hum Mutat **16**(5): 386-394.

- Ogata, S., I. Ho, et al. (1995). "Tumor-associated sialylated antigens are constitutively expressed in normal human colonic mucosa." Cancer Res **55**(9): 1869-1874.
- Prien, J. M., D. J. Ashline, et al. (2009). "The high mannose glycans from bovine ribonuclease B isomer characterization by ion trap MS." J Am Soc Mass Spectrom **20**(4): 539-556.
- Prien, J. M., L. C. Huysentruyt, et al. (2008). "Differentiating N-linked glycan structural isomers in metastatic and nonmetastatic tumor cells using sequential mass spectrometry." Glycobiology **18**(5): 353-366.
- Rademacher, T. W., R. B. Parekh, et al. (1988). "Glycobiology." Annu Rev Biochem **57**: 785-838.
- Ruddock, L. W. and M. Molinari (2006). "N-glycan processing in ER quality control." J Cell Sci **119**(Pt 21): 4373-4380.
- Schachter, H. (2004). "Protein glycosylation lessons from *Caenorhabditis elegans*." Curr Opin Struct Biol **14**(5): 607-616.
- Schollen, E., S. Kjaergaard, et al. (2004). "Increased recurrence risk in congenital disorders of glycosylation type Ia (CDG-Ia) due to a transmission ratio distortion." J Med Genet **41**(11): 877-880.
- Tkacz, J. S. and O. Lampen (1975). "Tunicamycin inhibition of polyisoprenyl N-acetylglucosaminyl pyrophosphate formation in calf-liver microsomes." Biochem Biophys Res Commun **65**(1): 248-257.
- Trent, C., N. Tsuing, et al. (1983). "Egg-laying defective mutants of the nematode *Caenorhabditis elegans*." Genetics **104**(4): 619-647.
- Unligil, U. M. and J. M. Rini (2000). "Glycosyltransferase structure and mechanism." Curr Opin Struct Biol **10**(5): 510-517.
- Varki, A. (1993). "Biological roles of oligosaccharides: all of the theories are correct." Glycobiology **3**(2): 97-130.
- Warren, C. E., A. Krizus, et al. (2002). "The *Caenorhabditis elegans* gene, gly-2, can rescue the N-acetylglucosaminyltransferase V mutation of Lec4 cells." J Biol Chem **277**(25): 22829-22838.